

# Temperature-Dependent Re-alignment of the Short Multifunctional Peptide BP100 in Membranes Revealed by Solid-State NMR Spectroscopy and Molecular Dynamics Simulations

Erik Strandberg<sup>+</sup>,<sup>\*,[a]</sup> Parvesh Wadhvani<sup>+</sup>,<sup>[a]</sup> Jochen Bürck,<sup>[a]</sup> Patrick Anders,<sup>[b]</sup> Christian Mink,<sup>[b, f]</sup> Jonas van den Berg,<sup>[b]</sup> Raffaele A. M. Ciriello,<sup>[b]</sup> Manuel N. Melo,<sup>[c, g]</sup> Miguel A. R. B. Castanho,<sup>[c]</sup> Eduard Bardají,<sup>[d]</sup> Jakob P. Ulmschneider,<sup>[e]</sup> and Anne S. Ulrich<sup>\*,[a, b]</sup>

BP100 is a cationic undecamer peptide with antimicrobial and cell-penetrating activities. The orientation of this amphiphilic  $\alpha$ -helix in lipid bilayers was examined under numerous conditions using solid-state  $^{19}\text{F}$ ,  $^{15}\text{N}$  and  $^2\text{H}$  NMR. At high temperatures in saturated phosphatidylcholine lipids, BP100 lies flat on the membrane surface, as expected. Upon lowering the temperature towards the lipid phase transition, the helix is found to flip into an upright transmembrane orientation. In thin bilayers,

this inserted state was stable at low peptide concentration, but thicker membranes required higher peptide concentrations. In the presence of lysolipids, the inserted state prevailed even at high temperature. Molecular dynamics simulations suggest that BP100 monomer insertion can be stabilized by snorkeling lysine side chains. These results demonstrate that even a very short helix like BP100 can span (and thereby penetrate through) a cellular membrane under suitable conditions.

[a] Dr. E. Strandberg,<sup>+</sup> Dr. P. Wadhvani,<sup>+</sup> Dr. J. Bürck, Prof. Dr. A. S. Ulrich  
Karlsruhe Institute of Technology (KIT)  
Institute of Biological Interfaces (IBG-2), POB 3640  
76021 Karlsruhe (Germany)  
E-mail: anne.ulrich@kit.edu

[b] Dr. P. Anders, Dr. C. Mink, Dr. J. van den Berg, R. A. M. Ciriello,  
Prof. Dr. A. S. Ulrich  
Karlsruhe Institute of Technology (KIT)  
Institute of Organic Chemistry  
Fritz-Haber-Weg 6, 76131 Karlsruhe (Germany)

[c] Dr. M. N. Melo, Prof. Dr. M. A. R. B. Castanho  
Instituto de Medicina Molecular  
Faculdade de Medicina, Universidade de Lisboa  
1649-028 Lisbon (Portugal)

[d] Prof. Dr. E. Bardají  
LIPPSO, Department of Chemistry  
University of Girona, Campus Montilivi  
17071 Girona (Spain)

[e] Prof. Dr. J. P. Ulmschneider  
Institute of Natural Sciences and  
School of Physics and Astronomy  
Shanghai Jiao Tong University  
Shanghai 200240 (China)

[f] Dr. C. Mink  
Present address: Syngenta Crop Protection AG  
4333 Münchwilen (Switzerland)

[g] Dr. M. N. Melo  
Present address: ITQB  
Instituto de Tecnologia Química e Biológica António Xavier  
Universidade Nova de Lisboa  
Av. da República, 2780-157 Oeiras (Portugal)

[†] These authors contributed equally to this work.

Supporting information for this article is available on the WWW under  
<https://doi.org/10.1002/cbic.202200602>

This article belongs to a Joint Special Collection dedicated to Ulf Diederichsen.

© 2022 The Authors. ChemBioChem published by Wiley-VCH GmbH. This is an open access article under the terms of the Creative Commons Attribution License, which permits use, distribution and reproduction in any medium, provided the original work is properly cited.

## Introduction

Cationic peptides, which can form amphipathic  $\alpha$ -helices with one charged face and one hydrophobic face, often show a membrane-permeabilizing activity and have been proposed as antimicrobial agents against multiresistant bacteria and other pathogens.<sup>[1–5]</sup> Numerous membrane-active peptides have been studied with biophysical methods to understand their detailed interactions with lipid bilayers, and many different mechanisms have been proposed, from pore-forming to micellization, and to the carpet mechanism.<sup>[2,4–5]</sup> In general, amphipathic helices tend to bind preferentially to membrane surfaces, that is, in a flat orientation with charged residues pointing toward the aqueous phase and hydrophobic residues pointing into the membrane interior; we call this the surface state (S-state). However, peptides may also form oligomeric pores by taking on a transmembrane orientation, with their charged residues pointing into the water-filled pore. This we call the inserted state (I-state). By examining the helix orientation in the membrane – for example, using solid-state NMR spectroscopy<sup>[6–9]</sup> or oriented circular dichroism (OCD)<sup>[10–11]</sup> – it is possible to see whether a peptide can assume a transmembrane alignment. A stable I-state is usually considered to be highly relevant in terms of the mechanistic model, as it is taken to represent the critical stage of pore formation. So far, most amphiphilic peptides have only been reported to exist in the S-state, and pore formation is at most speculated to occur transiently in the course of membrane attack. It is important to realize, however, that different model membranes and experimental conditions strongly influence the peptide alignment, hence it is critical to screen numerous lipids and parameters in order to understand whether and under

which conditions an inserted helix may be stable, so that it can then be structurally characterized in a comprehensive manner.

One factor that affects the peptide-lipid interactions is concentration. At low peptide concentrations, all amphipathic helices can be expected to prefer the surface state, since a pore should be formed by several peptides and a certain concentration is needed for peptides to have a high probability of self-assembly. From concentration-dependent orientation and activity studies, it is possible to deduce how strong these peptide-peptide interactions are.<sup>[12]</sup>

Another important factor is spontaneous bilayer curvature. This is related to the shape of the lipid molecules that make up the membrane. A lipid with a small head group and large acyl chain region (a cone shape), for example, a phosphatidylethanol (PE) lipid, exerts a negative spontaneous curvature in the bilayer. It has been shown that this favors the surface state of amphipathic peptides,<sup>[13]</sup> as expected from the “free” volume between the lipid head groups where the peptide helix can be readily accommodated. Lipids with a large head group and small acyl chain region (an inverted cone shape), for example, a lysolipid, have a positive spontaneous curvature, which in turn favors the transmembrane state of amphipathic peptides.<sup>[13]</sup> Lipids with a spontaneous curvature close to zero (a cylindrical shape), for example, 1,2-dimyristoyl-*sn*-glycero-3-phosphatidylcholine (DMPC), can allow different orientation states.

In solid-state NMR studies, it has been observed that all tested amphipathic peptides are in the surface state when using lipid systems composed of 1-palmitoyl-2-oleoyl-*sn*-glycero-3-phosphatidylcholine (POPC), 1-palmitoyl-2-oleoyl-*sn*-glycero-3-phosphatidylglycerol (POPG), or 1-palmitoyl-2-oleoyl-*sn*-glycero-3-phosphatidylethanolamine (POPE).<sup>[13]</sup> From this, it should be clear that this state is mostly due to lipid properties, rather than reflecting any particular features of the peptide. Such a result cannot be taken to exclude the possibility that a peptide operates via a pore-forming mechanism in a genuine bacterial membrane consisting of a much more complex lipid mixture. On the other hand, in model membranes containing lysolipids, a transmembrane state is often found to be favored, hence a transmembrane orientation in such a lipid system cannot by itself be taken as proof that a peptide forms stable pores in a biological membrane. Nonetheless, if there are reasons to believe from other experiments that a peptide acts by forming pores, it should be very useful to find a model system that supports thermodynamically stable pores, to be able to study the structure of these pores in more detail.

Cationic  $\alpha$ -helical AMPs, such as the designed sequence MSI-103 with 21 residues [(KIAGKIA)<sub>3</sub>-NH<sub>2</sub>],<sup>[14]</sup> have been proposed to form pores in membranes with peptides in a transmembrane orientation lining a water-filled pore. MSI-103 analogs, called KIA peptides, were used to investigate the length-dependent membrane-perturbing activity of such peptides. It was found that peptides must be long enough to span the membrane to be active, and this length dependence was observed for both, antimicrobial and hemolytic activity, as well as for vesicle leakage.<sup>[15]</sup> To kill *Escherichia coli* bacteria and cause leakage in POPC/POPG vesicles, at least 17 amino acids needed to fold into a helix such that its length is well matched

to the hydrophobic thickness of the bilayer.<sup>[15]</sup> The presence of charges on the termini of the helix were shown to influence leakage in a way that is fully consistent with peptide insertion and hence a pore-forming mechanism.<sup>[16]</sup> We have recently shown that stable KIA pores can be prepared in the presence of lysolipids. Solid-state <sup>15</sup>N NMR spectroscopy was used to characterize the transmembrane peptide orientation for MSI-103 analogs of different lengths.<sup>[17]</sup> It could be demonstrated that the formation of toroidal pores is a cooperative process involving several peptides, and that these pores are enriched in lysolipids.<sup>[18]</sup>

Seventeen amino acids was the minimum length for KIA peptides to span the membrane of POPC/POPG vesicles and kill *E. coli*. However, another peptide, BP100, with only 11 amino acids,<sup>[19,20]</sup> can also efficiently kill *E. coli* and induce leakage in POPC/POPG vesicles.<sup>[21,22]</sup> This short amphipathic peptide is highly helical in the presence of membranes. It is a multifunctional peptide that is not only a good AMP with broad-spectrum activity against Gram-positive and Gram-negative bacteria with relatively small hemolytic side effects, but it is at the same time also an efficient cell-penetrating peptide.<sup>[19,21–24]</sup> As evidenced from vesicle leakage studies, BP100 can target and permeabilize the membrane. BP100 is clearly too short to span a biological membrane, so it is unlikely to form pores such as those proposed for the KIA peptides. Indeed, studies using solid-state NMR and OCD have so far always found BP100 to reside either flat on the bilayer surface – also under conditions where KIA21 is in a transmembrane state – or it is at most found to be slightly tilted in the membrane.<sup>[21,22]</sup> It was therefore proposed that BP100 does not form pores but instead operates via a carpet mechanism, wherein peptide binding to the surface of the outer monolayer leads to permeabilization and rupture of the cell membrane.<sup>[21,22]</sup> Nonetheless, it is still conceivable that short-lived pores might form only transiently, which are not stable enough to be trapped and observed using NMR or OCD under the conditions studied so far.

Here, we used BP100 as a representative peptide to further investigate factors affecting the orientation of short amphiphilic helices in membranes. Using a combination of solid-state NMR methods and OCD, the intention was to extend previous studies and test shorter lipids, higher peptide concentrations, and lower temperatures, using a combination of different NMR methods under these conditions. Remarkably, we found conditions under which BP100 is fully inserted into the bilayer in an upright I-state, indicating that it is also possible for this very short peptide to have a stable transmembrane orientation under suitable conditions. Given the wide polar angle of BP100 (see helical wheel in Figure 1A) and high density of positive charges (5 Lys, cationic N terminus, amidated C terminus), it was questionable whether an oligomeric state would be stable at all. Molecular dynamics simulations were thus conducted on a BP100 monomer to examine possible helix orientations in a model membrane. It was found that a BP100 peptide can take on a stable transmembrane orientation by snorkeling, that is, by stretching out its charged lysine side chains to both sides of the membrane.

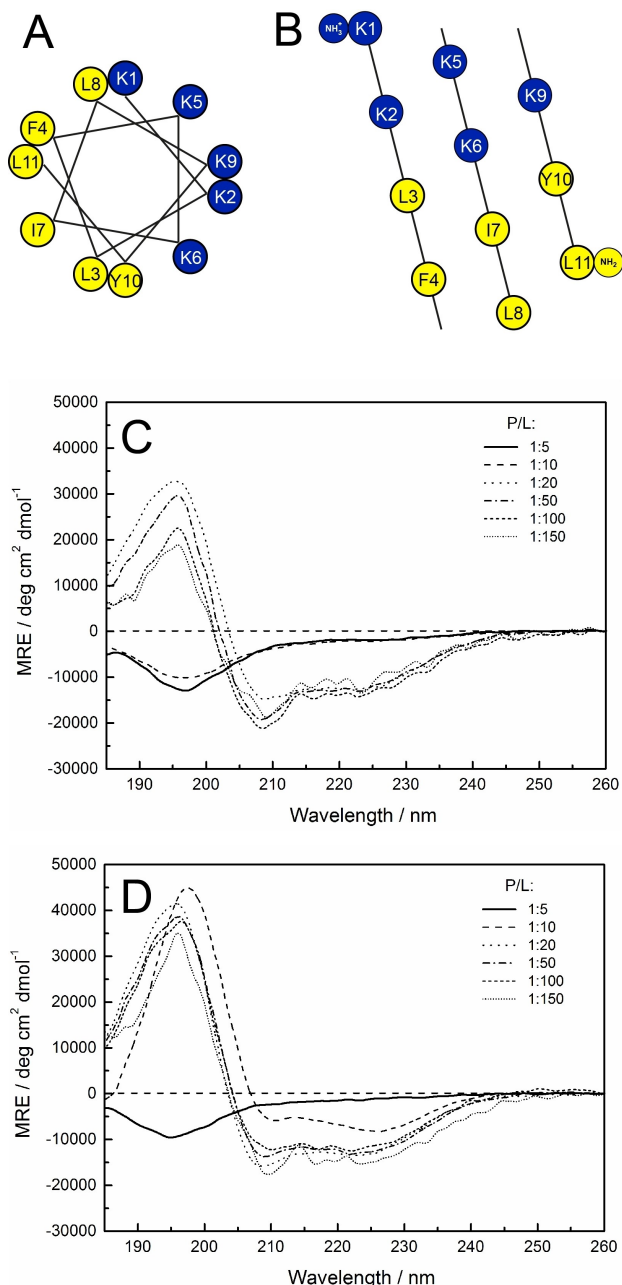


**Figure 1.** A) Helical wheel and B) helical mesh representations of BP100 prepared using the Protein Origami web application.<sup>[34]</sup> C) CD spectra of BP100 in weakly charged DMPC/DMPG (3:1) vesicles at different P/L ratios. The disordered peptide in solution is electrostatically attracted to the vesicles and forms an  $\alpha$ -helix when bound to the membranes. At high P/L (1:10 and 1:5), the charge of the vesicles is too low to attract all peptides, so a random-coil signal is observed. D) CD spectra at different P/L ratios in predominantly anionic DMPC/DMPG (1:3), showing that a random-coil signal remains only at P/L = 1:5 when electroneutrality is not yet met.

## Experimental Section

**Peptide synthesis:** Peptides were synthesized using a standard Fmoc solid phase protocol.<sup>[22,25]</sup>

**Minimum inhibitory concentration (MIC) assay:** The antimicrobial activity of BP100 and its <sup>19</sup>F-labeled analogs was tested using a

standard MIC dilution assay with four replicates, as previously described.<sup>[22,26]</sup>

**Circular dichroism spectroscopy (CD) and oriented CD (OCD):** Details of BP100 sample preparation in lipid vesicles and in oriented lipid bilayers, as well as for CD/OCD measurements, have been described in a recent paper.<sup>[22]</sup> CD samples were prepared from 300  $\mu$ M peptide stock solution in water and added to a DMPC/1,2-dimyristoyl-*sn*-glycero-3-phosphatidylglycerol (DMPG; 3:1 molar ratio) liposome dispersion in 10 mM phosphate buffer (PB, pH 7.0). The final peptide concentration in the liposome samples was adjusted in the range of 15–75  $\mu$ M, while the lipid concentration was varied between 0.3–2.2 mM, resulting in peptide-to-lipid molar ratios (P/L) of 1:5, 1:10, 1:20, 1:50, 1:100 and 1:150. The peptide concentration in the stock solution was determined from the UV absorption of a single Tyr residue at 280 nm.<sup>[22,27]</sup> The concentration of the final CD samples was calculated from the respective dilution factors. The measured CD spectra were converted to mean residue ellipticities by using these peptide concentrations and the 0.1 cm path length of the cuvette.

After the CD measurements, aliquots of the vesicle samples were deposited as a circular spot of 12 mm diameter on quartz glass plates, dried and rehydrated in the OCD chamber overnight to obtain oriented lipid bilayer samples, as described previously.<sup>[28]</sup> A saturated salt solution of K<sub>2</sub>SO<sub>4</sub> was placed in the OCD chamber to reach a high hydration of  $\sim$ 96.7% relative humidity (rH), and solutions of LiCl, MgCl<sub>2</sub> and NaCl were used to reach lower humidities of 11.3% rH, 32.1% rH and 74.9% rH according to the literature values,<sup>[29]</sup> although the values measured by a sensor inside the OCD chamber were  $\sim$ 23% rH,  $\sim$ 43% rH and  $\sim$ 80% rH, respectively. The CD and OCD spectra of all samples were recorded at 35 °C according to the protocols described in refs. [22] and [28].

**Solid-state NMR:** Solid-state <sup>31</sup>P, <sup>2</sup>H, <sup>19</sup>F, and <sup>15</sup>N NMR studies of lipid-peptide samples macroscopically oriented on glass plates were performed as previously described in detail.<sup>[21,22,30]</sup>

**MD simulations:** Molecular dynamics simulations were performed as described previously.<sup>[31]</sup>

## Results

### Peptide synthesis

Peptides were synthesized using a standard Fmoc solid phase protocol. In addition to the original BP100 peptide (below also called BP100-wt), specific <sup>2</sup>H, <sup>15</sup>N, or <sup>19</sup>F isotope labels were incorporated for solid-state NMR studies. One peptide contained a <sup>15</sup>N-label at Leu8, and six peptides were selectively <sup>19</sup>F-labeled with a single CF<sub>3</sub>-Bpg [3-(trifluoromethyl)-L-bicyclopent-[1.1.1]-1-ylglycine] residue each<sup>[32–33]</sup> at Leu3, Phe4, Ile7, Leu8, Tyr10, or Leu11, as previously described.<sup>[22]</sup> In addition, 11 peptides were prepared where each position was replaced, one at a time, with <sup>2</sup>H-labeled [D<sub>3</sub>]Ala as previously described.<sup>[21]</sup> All peptides used are listed in Table 1.

### Circular dichroism

Circular dichroism spectroscopy is readily used to monitor the folding of unstructured peptides into  $\alpha$ -helical structures, and it can yield information on the binding of soluble peptides to

**Table 1.** Sequences of used peptides.

| Peptide                   | Sequence  |
|---------------------------|---|
| BP100                     | KKLFFKILKYL-NH <sub>2</sub>                       |
| BP100-8L- <sup>15</sup> N | KKLFFKIL- <sup>15</sup> N-Leu-KYL-NH <sub>2</sub> |
| BP100-3L-Bpg              | KK-CF <sub>3</sub> -Bpg-FKKILKYL-NH <sub>2</sub>  |
| BP100-4F-Bpg              | KKL-CF <sub>3</sub> -Bpg-KKILKYL-NH <sub>2</sub>  |
| BP100-7I-Bpg              | KKLFFK-CF <sub>3</sub> -Bpg-LKYL-NH <sub>2</sub>  |
| BP100-8L-Bpg              | KKLFFKIL-CF <sub>3</sub> -Bpg-KYL-NH <sub>2</sub> |
| BP100-10Y-Bpg             | KKLFFKILK-CF <sub>3</sub> -Bpg-L-NH <sub>2</sub>  |
| BP100-11L-Bpg             | KKLFFKILKY-CF <sub>3</sub> -Bpg-NH <sub>2</sub>   |
| BP100K1A                  | [D <sub>3</sub> ]Ala-KLFFKILKYL-NH <sub>2</sub>   |
| BP100K2A                  | K-[D <sub>3</sub> ]Ala-LFFKILKYL-NH <sub>2</sub>  |
| BP100L3A                  | KK-[D <sub>3</sub> ]Ala-FKKILKYL-NH <sub>2</sub>  |
| BP100F4A                  | KKL-[D <sub>3</sub> ]Ala-KKILKYL-NH <sub>2</sub>  |
| BP100K5A                  | KKLF-[D <sub>3</sub> ]Ala-KILKYL-NH <sub>2</sub>  |
| BP100K6A                  | KKLFFK-[D <sub>3</sub> ]Ala-ILKYL-NH <sub>2</sub> |
| BP100I7A                  | KKLFFK-[D <sub>3</sub> ]Ala-LKYL-NH <sub>2</sub>  |
| BP100L8A                  | KKLFFKIL-[D <sub>3</sub> ]Ala-KYL-NH <sub>2</sub> |
| BP100K9A                  | KKLFFKIL-[D <sub>3</sub> ]Ala-YL-NH <sub>2</sub>  |
| BP100Y10A                 | KKLFFKILK-[D <sub>3</sub> ]Ala-L-NH <sub>2</sub>  |
| BP100L11A                 | KKLFFKILKY-[D <sub>3</sub> ]Ala-NH <sub>2</sub>   |

lipid vesicles. CD has been previously used to show that BP100 forms a random coil in solution but is helical when bound to membranes. In the presence of DMPC/DMPG (3:1) at P/L = 1:100, the BP100-wt configuration was reported to be over 60%  $\alpha$ -helix.<sup>[22]</sup> Here, we acquired an extended series of concentration-dependent CD spectra for BP100 in DMPC/DMPG (3:1) vesicles, with P/L = 1:150, 1:100, 1:50, 1:20, 1:10, and 1:5. The data in Figure 1C show that BP100 is always  $\alpha$ -helical, except for very high P/L values of 1:10 and 1:5, where it remains largely disordered. This observation suggests that charged lipids are essential for attracting cationic BP100 to vesicles. With a charge of +6 on BP100 and 25% anionic lipids in the vesicles, there are enough negative charges on the vesicles to match the charges of the peptides up to P/L = 1:24. However, at P/L = 1:10 and 1:5, most peptides remain unbound and show a random coil CD line shape. When the same experiment was repeated in DMPC/DMPG (1:3), that is, with 75% anionic lipids (Figure 1B), a random coil was observed only for P/L = 1:5, which fits the estimated limit for electroneutrality.

### Oriented CD

Oriented CD on macroscopically aligned membrane samples is a powerful tool for examining the alignment of helical peptides in oriented membranes.<sup>[10,11,28]</sup> This sensitive method has been used to monitor the concentration-dependent realignment of various long amphiphilic AMPs in lipid bilayers, which is functionally relevant in terms of pore formation.<sup>[10,28,35,36]</sup> Oriented CD was also performed in our earlier study of BP100, specifically in DMPC/DMPG (3:1) bilayers at P/L = 1:100, 1:25, and 1:12.5.<sup>[22]</sup> In all cases, the helix was found to lie essentially flat on the membrane surface. However, given that some other amphipathic helical peptides showed important rearrangements only at very high concentrations, here we tried a wider range of P/L values, including P/L = 1:150, 1:100, 1:50, 1:20, 1:10, and 1:5 (Figure S1A in the Supporting Information), but

hardly any difference was found in these spectra, so no significant change in orientation could be detected for BP100 as a function of peptide concentration in DMPC/DMPG at 30 °C.

In previous studies, the orientations of several peptides were found to change with the humidity of the sample, again with functionally relevant implications for pore formation.<sup>[36–38]</sup> Therefore, OCD samples of BP100 were prepared with different relative humidities (using DMPC/DMPG at P/L = 1:100) of 23.4, 43.0, 80.0, or 96.7%. However, this series (Figure S1B) also showed hardly any change, indicating that BP100 remained flat on the membrane surface of DMPC/DMPG, independent of sample hydration. Finally, we compared the method of preparing the OCD samples (DMPC/DMPG, P/L = 1:100) either from an aqueous suspension of vesicles or from co-dissolved peptides and lipids in organic solvents (CHCl<sub>3</sub>/MeOH/H<sub>2</sub>O). This had no influence either on the peptide orientation (Figure S1C). We can thus conclude that the orientation of BP100 in DMPC/DMPG membranes at 30 °C is independent of peptide concentration, sample hydration, or the method of sample preparation.

### Solid-state NMR spectroscopy

To be able to observe and interpret several orthogonal NMR parameters unambiguously, we combined three NMR isotopes to monitor the orientation of BP100 in membranes as a function of several factors. <sup>15</sup>N NMR spectroscopy on peptides labeled at a single position can give an approximate tilt angle (the angle between the helix long axis and the membrane normal) from a single 1D spectrum. From a series of peptides that are selectively labeled with <sup>2</sup>H or <sup>19</sup>F at the side chains, the peptide conformation and its membrane alignment and dynamic behavior can be determined with high accuracy, and this method has been used by our group to study many different types of membrane-active peptides.<sup>[32,39–53]</sup> The <sup>2</sup>H/<sup>19</sup>F NMR approach is very sensitive to structural changes, giving not only a full 3D picture of the peptide orientation in terms of the tilt angle and the azimuthal angle (which defines the rotation around the helix axis), which can be determined with high accuracy but also addressing a wider range of concentrations compared to OCD or <sup>15</sup>N NMR. Labeling a peptide with CF<sub>3</sub>-Bpg or [D<sub>3</sub>]Ala can lead to changes in its function; therefore, antimicrobial tests were performed on the modified peptides. [D<sub>3</sub>]Ala-labeled peptides had been previously tested against four types of bacteria, and it was found that the activity was somewhat reduced when the hydrophobic residues were replaced by [D<sub>3</sub>]Ala, but not when Lys was replaced.<sup>[21]</sup> Here, we tested all <sup>19</sup>F-labeled peptides against *E. coli*, *E. helveticus*, and *K. rhizophila* and found a high activity against all three bacteria for all labeled peptides, similar to or even better than that for BP100-wt (Table S1). BP100 and its <sup>19</sup>F-labeled analogs also showed high activities against plant-pathogenic *E. amylovora*, *P. syringae*, and *X. axonopodis* (Table S2). We can thus conclude that the <sup>2</sup>H and <sup>19</sup>F labels did not interfere with the antimicrobial function.

### <sup>19</sup>F NMR spectroscopy

The main advantage of <sup>19</sup>F as an NMR nucleus is its high sensitivity combined with low background signals. Thus, small amounts of labeled peptide and short experimental times can be used, and <sup>19</sup>F NMR is therefore very useful for scanning a range of conditions. We had previously placed a CF<sub>3</sub>-Bpg label at position Ile7 and reconstituted the peptide in samples with a wide range of P/L ratios from 1:3000 to 1:10 in DMPC/DMPG (3:1),<sup>[22]</sup> which would not have been possible using other NMR methods or OCD. In the fluid phase (at 35 °C) the <sup>19</sup>F dipolar splitting remained the same, meaning that the peptide does not change its orientation or dynamics as a function of concentration in the membrane, which was also observed by the concentration-dependent OCD measurements. As many other antimicrobial peptides are known to change their alignment under various conditions,<sup>[35,42,48,51,54]</sup> we had monitored the <sup>19</sup>F NMR splittings in many different lipid compositions at 40 °C.<sup>[30]</sup> However, no re-alignment of BP100 was observed when comparing zwitterionic DMPC (di-C12:0 acyl chains) with anionic DMPC/DMPG mixtures, nor with thin 1,2-dilauroyl-*sn*-glycero-3-phosphatidylcholine (DLPC, di-C12:0 acyl chains) bilayers, thick 1,2-dierucoyl-*sn*-glycero-3-phosphatidylcholine (DERPC, di-C22:1 acyl chains) bilayers, or in the branched-chain lipid 1,2-diphytanoyl-*sn*-glycero-3-phosphatidylcholine (DPHPC, characteristic of archaea) at P/L = 1:100.<sup>[30]</sup> Other studies in DMPC in the presence of cholesterol (characteristic of eukaryotic membranes), as well as in membranes extracted from erythrocytes and *M. luteus*, at P/L = 1:20, have also reported the same stable surface-alignment of BP100.<sup>[30]</sup>

Here, we studied the effect of temperature, which has previously been observed to have an effect on the orientation of PGLa, a helical AMP with 21 amino acids.<sup>[46]</sup> For PGLa in DMPC at P/L = 1:50, a surface-bound state was observed at high temperatures, an inserted state was observed in the gel phase, and an aggregated state was observed at even lower temperatures in crystalline lipids.<sup>[46]</sup> <sup>19</sup>F NMR spectroscopy was thus performed on BP100 labeled at six different positions with CF<sub>3</sub>-Bpg and reconstituted in DMPC/DMPG (3:1) and DLPC/DLPG (3:1) at a P/L of 1:100. Temperatures were addressed both above and below the corresponding gel-to-liquid crystalline phase transition temperatures (*T<sub>m</sub>*). The full sets of <sup>19</sup>F NMR spectra are shown in Figure S2, collected on oriented samples that were positioned with the bilayer normal parallel to the magnetic field (0° sample angle). The splittings of the six different labels are listed in Tables S3 and S4. At 35 °C, above the *T<sub>m</sub>*, the splittings are very similar in the two lipid systems, and peptides are observed to be flat on the membrane surface. Below *T<sub>m</sub>*, at 15 °C in DMPC/DMPG (with a *T<sub>m</sub>* of 25 °C) and at -20 °C in DLPC/DLPG (with a *T<sub>m</sub>* of 5 °C), the spectra are broader, but the splittings are quite similar to those above the *T<sub>m</sub>*. We can thus conclude that also in the gel phase BP100 prefers to be oriented flat on the membrane surface. The oriented samples were also measured with the bilayer normal perpendicular (90° sample angle) to the external magnetic field, in order to assess the peptide dynamics. <sup>19</sup>F NMR spectra at both, 0° and 90° sample angles, are given in Figures S3–S5, as

well as <sup>31</sup>P NMR spectra which show that the lipids are well oriented in all samples. It is also seen that in the liquid crystalline phase, the <sup>19</sup>F NMR splittings at a 90° sample angle are scaled by a factor of -1/2 compared to the 0° measurements, which indicates fast rotational diffusion of peptides in the membrane. In the gel phase, peptides are immobilized, as seen from the powder-like splittings of approximately -7.5 kHz in the samples measured at 90° angle.

The above set of samples had a relatively low peptide concentration (P/L = 1:100), so we performed further experiments with higher P/L ratios, again over a wide range of temperatures around the respective *T<sub>m</sub>*. For BP100-3L-Bpg in DLPC at P/L = 1:25, the temperature was changed in steps of 5 °C from 35 to -15 °C. The corresponding spectra measured with the oriented samples set at a 0° angle are shown in Figure 2. At 35 °C, the splitting is close to 0 kHz, and only a single peak is observed. At lower temperatures, however, there is a change in the splitting. Below 10 °C, a triplet with a splitting of -4.6 kHz appears, and at -10 °C, a second set of peaks emerges with a splitting of -7.5 kHz, which dominates at lower temperatures. Besides these data on BP100 labeled at position Leu3, we also used two further labels, BP100-7I-CF<sub>3</sub>-Bpg and BP100-8L-CF<sub>3</sub>-Bpg, to examine the temperature-dependent effects observed here in thin DLPC bilayers. Interestingly, a similar behavior was observed for all three <sup>19</sup>F labels (Figures S6 and S7), as the splittings appearing at approximately 10 °C were quite different to those at 35 °C; while splittings of -7.5 kHz were observed below -10 °C. The latter splitting is typically seen for aggregated samples<sup>[42,55]</sup> or molecules that are otherwise immobilized.<sup>[30]</sup> Given the low temperature of the gel phase, this simply indicates that the peptides are immobilized

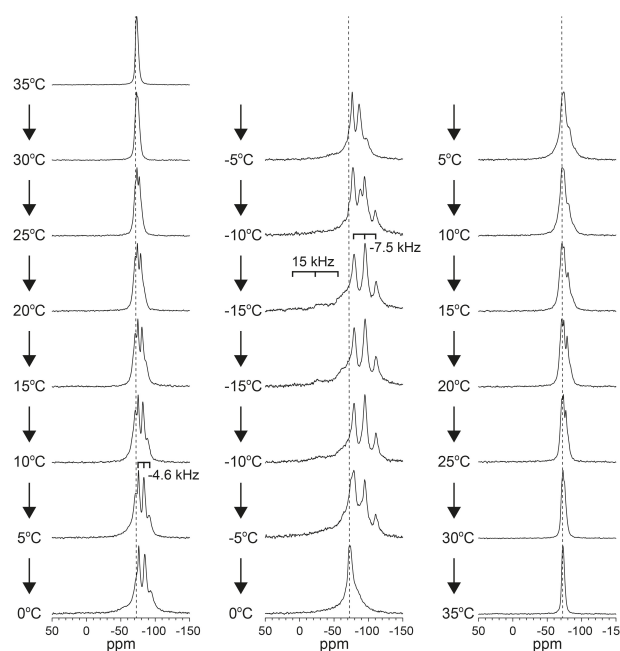


**Figure 2.** <sup>19</sup>F NMR spectra of BP100-3L-Bpg in DLPC at P/L = 1:25 and at different temperatures. The samples are oriented with the membrane normal parallel to the magnetic field.

at  $-10^{\circ}\text{C}$ , which was confirmed by the spectra measured at a  $90^{\circ}$  sample angle (Figures S8–S10).

It is readily seen from the  $^{19}\text{F}$  NMR spectra of BP100-8L-CF<sub>3</sub>-Bpg (Figures S7 and S10) that upon changing the sample angle from  $0^{\circ}$  to  $90^{\circ}$ , at temperatures above  $-10^{\circ}\text{C}$ , the splittings are scaled by a factor of  $-0.5$ , which is indicative of fast rotational diffusion of the peptides. Interestingly, at or below  $-10^{\circ}\text{C}$ , a splitting of  $-7.5$  kHz was found both for  $0^{\circ}$  and  $90^{\circ}$  angles of the samples for all three labeled peptides (Figures S8–S10), indicating immobilized peptides. We can thus conclude that the orientation of BP100 undergoes an interesting change when the temperature is lowered towards the respective  $T_m$ . Thereafter, at temperatures below  $T_m$ , the peptide is again surface-bound but immobilized.

### $^{15}\text{N}$ NMR spectroscopy

A straightforward method for monitoring the tilt angle of a helical peptide is to measure the NMR chemical shift of a  $^{15}\text{N}$ -label in the backbone of a helical peptide that is reconstituted in an oriented membrane sample. We had previously analyzed selectively  $^{15}\text{N}$ -labeled BP100-8L- $^{15}\text{N}$  in DMPC/DMPG (3:1) vesicles at  $P/L=1:50$ ,  $1:100$ , and  $1:200$  at  $35^{\circ}\text{C}$ , showing signals at approximately 92 ppm in all cases, indicating that the peptide lies flat on the membrane surface.<sup>[22]</sup> In a more recent study, we used a higher BP100 concentration,  $P/L=1:20$ , and performed measurements at  $35^{\circ}\text{C}$ . In bilayers of POPC/POPG (3:1 mol/mol), a signal at 89 ppm was found, and in DMPC/DMPG (3:1), the signal was at 95 ppm, also indicating that the peptides lie flat on the membrane surface under these conditions. Interestingly, in DMPC/DMPG/1-myristoyl-2-hydroxy-*sn*-glycero-3-phosphatidylcholine (lyso-MPC) (1:1:1), the signal was found to be moderately shifted to 137 ppm in liquid crystalline bilayers, indicating a more tilted orientation.<sup>[21]</sup> With the corresponding oblique angle, however, the helix was not tilted far enough to reflect a complete transmembrane alignment. The set of motionally averaged parameters could rather be attributed to a highly dynamical state of the peptide undergoing whole-body motion in these lysolipid containing membranes, with a time-averaged oblique membrane orientation.<sup>[21]</sup>

Here, we used the same  $^{15}\text{N}$ -labeled BP100-8L- $^{15}\text{N}$  peptide to find out how the intriguing temperature-dependent changes seen in the  $^{19}\text{F}$  NMR samples would show up in  $^{15}\text{N}$  NMR spectra, in order to quantify the underlying change in helix tilt angle. A temperature series of  $^{15}\text{N}$  NMR spectra was recorded in DLPC bilayers at  $P/L=1:20$ , both above and below the lipid phase transition temperature, that is between  $35^{\circ}\text{C}$  and  $-5^{\circ}\text{C}$ , as shown in Figure 3A. Indeed, a gradual shift of the peak position was observed. At  $35^{\circ}\text{C}$ , the peak was at 100 ppm, indicating a surface-bound state, whereas at  $-5^{\circ}\text{C}$ , the peak was found at 171 ppm, indicating a genuine transmembrane orientation of BP100. This is the first time we can confirm a stable transmembrane state of this short peptide in thin bilayers.

To find out the minimum peptide concentration needed to attain the transmembrane state,  $^{15}\text{N}$  NMR experiments were

also performed at lower peptide-to-lipid ratios. At  $P/L=1:40$  (Figure 3B), there was not a gradual shift, but instead a discrete flip in orientation. At or above  $15^{\circ}\text{C}$  a surface orientation was observed, whereas at 5 and  $0^{\circ}\text{C}$  a transmembrane orientation was observed. Eventually, at  $-5^{\circ}\text{C}$  the peak shifted back to 90 ppm, indicating again a surface-bound state below  $T_m$ , which was retained at  $-10^{\circ}\text{C}$ . Even at a low concentration of  $P/L=1:100$ , the transmembrane orientation could be detected, but only at  $5^{\circ}\text{C}$ , close to the  $T_m$  (Figure 3C).

It has been reported that peptide insertion in a transmembrane orientation is favored in lipid systems with a high positive spontaneous bilayer curvature, for example in lysolipids.<sup>[13,56–57]</sup> Further  $^{15}\text{N}$  NMR experiments were therefore performed in mixed bilayers of DLPC/1-lauroyl-2-hydroxy-*sn*-glycero-3-phosphatidylcholine (lyso-LPC; 2:1) at  $P/L=1:20$ . Here, the peptide peak was found at approximately 150 ppm at all temperatures from  $35^{\circ}\text{C}$  down to  $-10^{\circ}\text{C}$  (Figure 3D). In this lipid system, it seems that a transmembrane orientation is stable even at temperatures well above the lipid phase transition temperature, which in this mixed system is too low to be reached with our experimental setup (lysolipids tend to reduce  $T_m$ ; see below).

Now that a transmembrane orientation was found in thin DLPC membranes, the question was whether this orientation would also be possible in a thicker membrane system.  $^{15}\text{N}$  NMR experiments were performed in DMPC at  $P/L=1:20$  at a range of temperatures (Figure 4A). At  $35^{\circ}\text{C}$ , the signal was at 105 ppm, indicating an almost flat surface orientation, but at lower temperature the signal got shifted. At  $25^{\circ}\text{C}$ , close to the lipid phase transition, the signal was at 145 ppm, a highly tilted orientation. At  $20^{\circ}\text{C}$ , two peaks were found, one at 145 ppm and one at 80 ppm, indicating that there are two populations of peptides that are not in fast exchange: one population on the surface, and the other one more inserted. Then, at lower temperatures, where lipids were in the gel phase, the signal was shifted back all the way to 80 ppm. This extreme chemical shift indicates that in the gel phase, peptides are completely flat on the surface, as they are pushed out of the solidified membrane core. This means that also in the thicker DMPC bilayers, BP100 can be inserted into the membrane in a stable manner when the temperature is close to  $T_m$ . At  $P/L=1:100$  in DMPC (Figure 4B), however, such insertion was no longer observed, that is at low peptide concentration BP100 remains flat on the DMPC surface at all temperatures.

The effect of anionic lipids was examined in DMPC/DMPG (1:1) at  $P/L=1:20$ , but the results were the same as those for DMPC at  $P/L=1:20$ , with inserted peptides around  $T_m$  and surface-bound peptides at high and low temperatures (Figure 4C). Thus, the presence of charged lipids seems to have no significant effect on the alignment of BP100.

When a positive curvature was introduced in DMPC, on the other hand, that is in DMPC/lyso-MPC (2:1) at  $P/L=1:20$  (Figure 4D), the peptide was aligned in a transmembrane state at  $35^{\circ}\text{C}$ , as indicated by the signal at 145 ppm. When the temperature was reduced, the peak shifted gradually to 152 ppm at  $15^{\circ}\text{C}$ . At  $10^{\circ}\text{C}$  and below, the signal moved to 80 ppm, indicating a complete surface orientation in the lipid

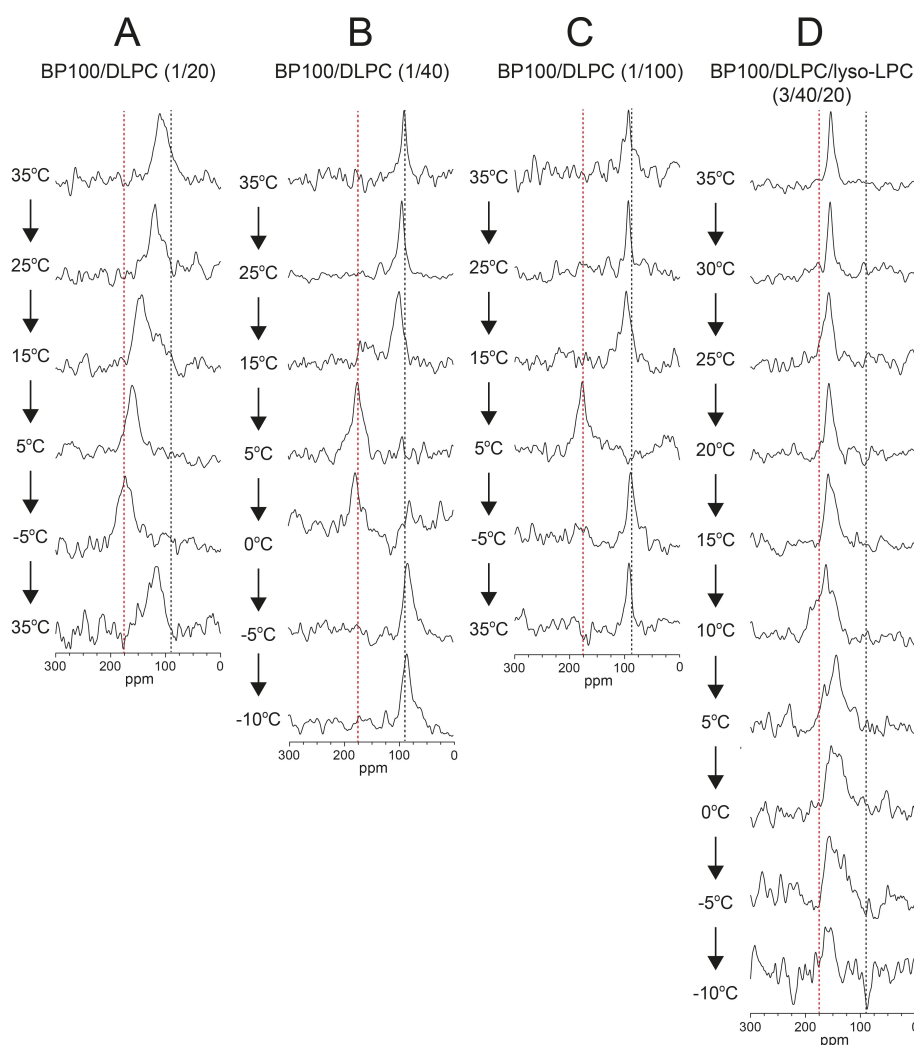


**Figure 3.**  $^{15}\text{N}$  NMR spectra of BP100-8L- $^{15}\text{N}$  measured in 12:0-PC lipids at a series of different temperatures above and below the lipid phase transition ( $T_m$  of DLPC  $\approx -5^\circ\text{C}$ ). The chemical shift of the peak indicates the orientation of the peptide. Signals at approximately 90 ppm (----) indicate peptides in a surface-aligned state. Signals at approximately 175 ppm (.....) indicate a complete transmembrane helix orientation. A) DLPC at P/L = 1:20; B) DLPC at P/L = 1:40; C) DLPC at P/L = 1:100; D) DLPC/lyso-LPC (2:1) at P/L = 1:20. Peak positions are listed in Table S5.

gel phase. The presence of lysolipids thus seems to lower the phase transition temperature from approximately  $25^\circ\text{C}$  to a value between  $10^\circ\text{C}$  and  $15^\circ\text{C}$ .

We thus conclude that at high peptide concentration, BP100 can assume an inserted transmembrane state in both DMPC and DLPC, at least at temperatures close to the respective  $T_m$ . In the presence of 33 mol% lysolipids, the peptide remains stable in the transmembrane state even at elevated temperatures. Since the chemical shift in DMPC is never higher than 145 ppm, whereas in DLPC it can reach 170 ppm, it seems that BP100 enters a completely upright, transmembrane orientation only in the thinner DLPC membranes. In DMPC, on the other hand, the time-averaged helix alignment is slightly slanted away from a perfectly upright transmembrane state, which might reflect some dynamical effects.

### $^2\text{H}$ NMR spectroscopy

Above, we had first used  $^{19}\text{F}$  NMR spectroscopy to screen numerous lipid compositions and temperature changes to detect particular conditions where significant spectral shifts occur. Then,  $^{15}\text{N}$  NMR was performed under those conditions to assign the helix alignment to a transmembrane inserted state in a qualitative manner. Finally, we could now use  $^2\text{H}$  NMR to obtain an accurate, 3D description of the orientation of BP100 in its transmembrane state. In previous analyses of BP100, comprehensive isotope labeling schemes had been systematically compared using  $^{19}\text{F}$  and  $^2\text{H}$  NMR spectroscopy.<sup>[21]</sup> It was found that the  $^2\text{H}$  NMR method worked better because all positions in the peptide could be labeled without disturbing the conformation or amphiphilic character, thus giving more data points for the data fit.<sup>[21]</sup> Here, we thus used  $^2\text{H}$  NMR to refine the transmembrane orientation of BP100 in terms of the helix tilt angle ( $\tau$ ) and its azimuthal rotation angle ( $\rho$ ), along

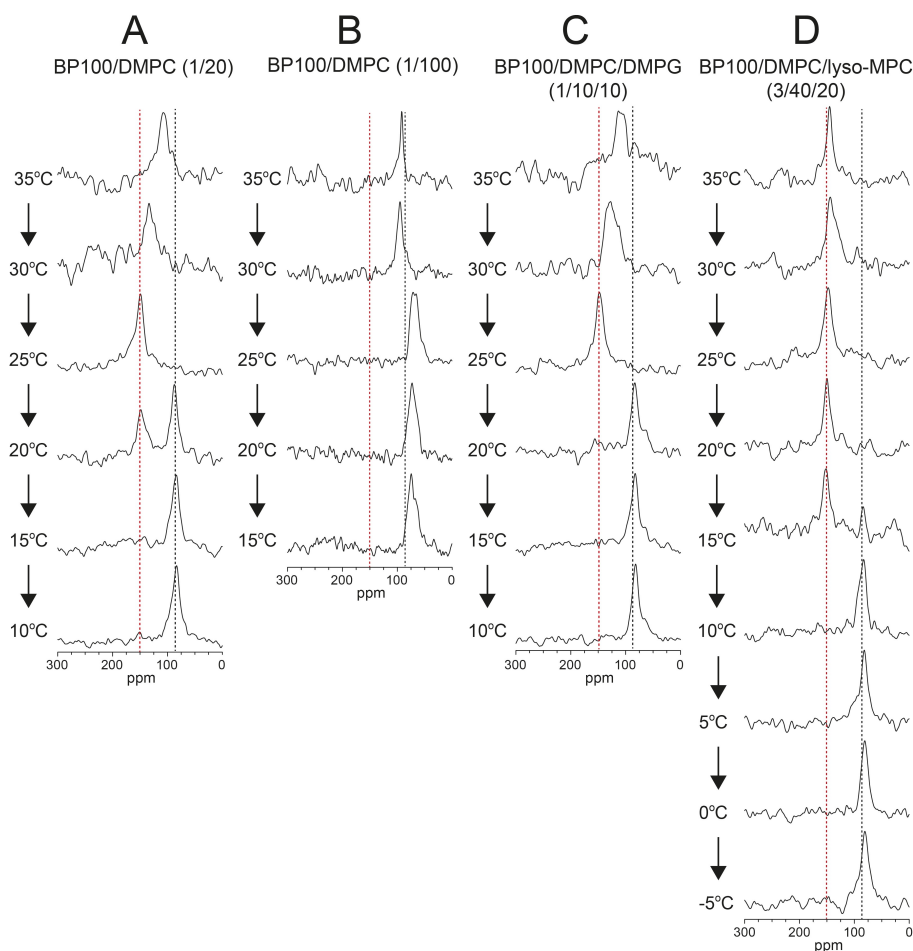


**Figure 4.**  $^{15}\text{N}$  NMR spectra of BP100-8L- $^{15}\text{N}$  measured in 14:0-PC lipids at a series of different temperatures above and below the lipid phase transition ( $T_m$  of DMPC  $\approx 25^\circ\text{C}$ ). The chemical shift of the peak indicates the orientation of the peptide. Signals at approximately 150 ppm (.....) indicate a strongly tilted state that is close to a transmembrane insertion. A) DMPC at P/L = 1:20; B) DMPC at P/L = 1:100; C) DMPC/DMPC (1:1) at P/L = 1:20; D) DMPC/lyso-MPC (2:1) at P/L = 1:20. Peak positions are listed in Table S5.

with the dynamical parameters ( $\sigma_\tau$  and  $\sigma_\rho$ ) describing the time-averaged fluctuations about these two axes. A detailed description of the spectral interpretation, the data analysis and the fitting procedures is found in our previous reports on BP100 in the surface-bound state.<sup>[21–22]</sup> In short, we compare the experimental  $^2\text{H}$  NMR splittings with so-called helical waves that are calculated for different values of the orientation angles and dynamical parameters. To determine the best-fit parameters, we systematically vary all parameters and search for that wave with the smallest deviation from the experimental data set. Based on the CD analysis showing that BP100 forms an  $\alpha$ -helix when bound to essentially any type of membrane, we can assume that the peptide is also helical in the NMR sample. Furthermore, once the fitting procedure has been performed, we can retrospectively deduce from the quality of the fit whether the peptide is indeed helical or not. That is because the splittings are very sensitive to small deviations in conformation and orientation, so if there is a good fit to the entire set of NMR data points (root mean square deviation, RMSD,  $< 3$  kHz) then the peptide must form an essentially perfect  $\alpha$ -helix over the full length of labeled positions.

BP100 was labeled with  $[\text{D}_3]\text{Ala}$  at each of its 11 positions, one at a time, and  $^2\text{H}$  NMR spectra were measured in oriented samples. Based on the above  $^{15}\text{N}$  NMR results, DLPC and DLPC/lyso-LPC were chosen as lipid systems, and measurements using P/L = 1:20 were performed at 35 and  $5^\circ\text{C}$ . The spectra in DLPC are shown in Figure 5. At  $35^\circ\text{C}$ , sharp peaks are observed and the splittings are easy to determine. In addition to the doublet from the  $[\text{D}_3]\text{Ala}$  label, there is often also a central peak from natural abundance deuterium in water. For position 3, there is only a central peak and it is assumed that the splitting from the peptide is close to 0. At  $5^\circ\text{C}$ , spectra show much broader lines, and for position 9, there is no clear splitting seen. For position 8, a small splitting is observed (marked in red in Figure 5; less line broadening was used in this case). Experiments were also performed at  $-5^\circ\text{C}$  for some peptides, but at this temperature, the spectra were of very low quality and could not be used for the analysis. The corresponding spectra in DLPC/lyso-LPC are shown in Figure 6.  $^2\text{H}$  NMR splittings are listed in Table 2, and data analysis results are shown in Figure 7 and summarized in Table 3.

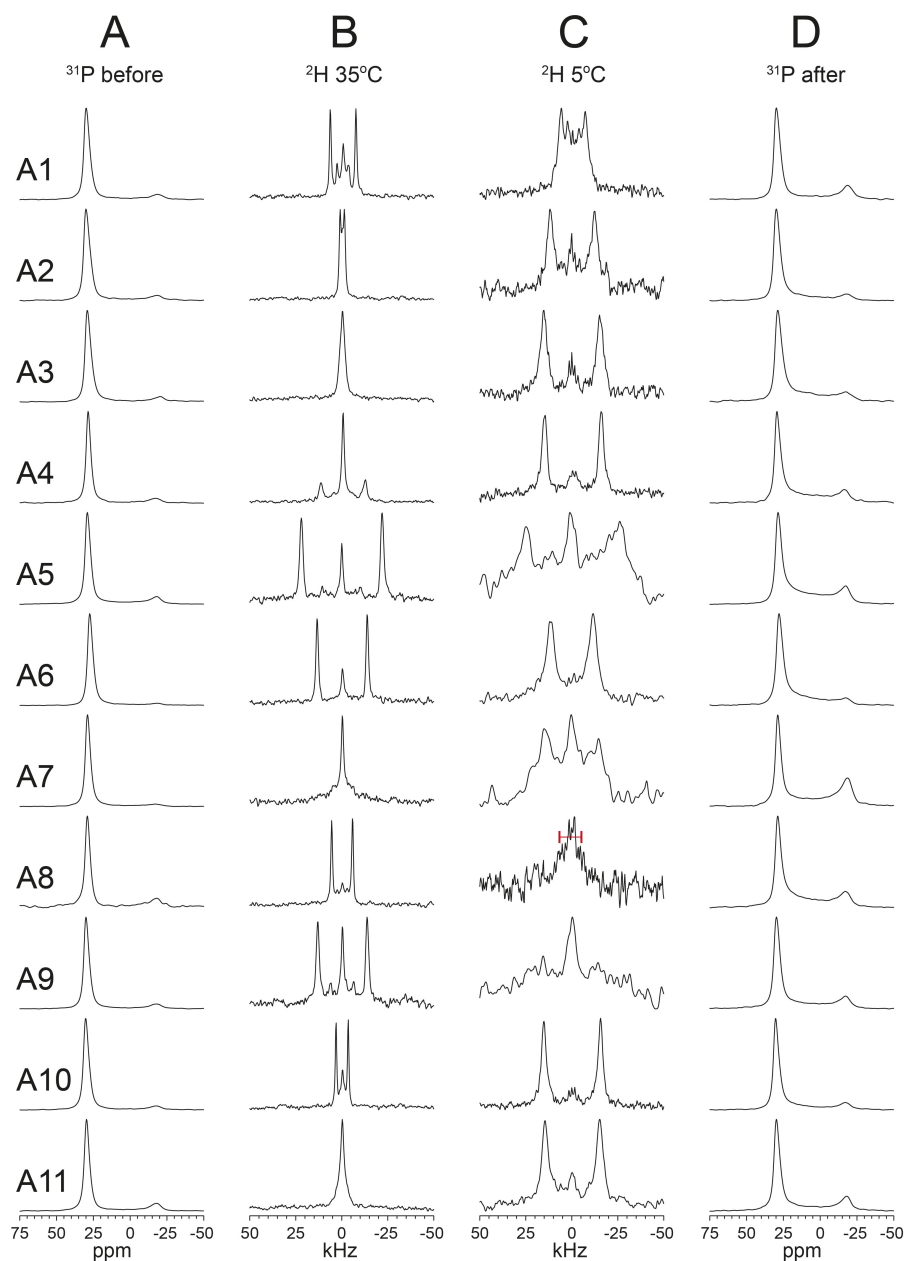


**Figure 5.**  $^2\text{H}$  NMR spectra of  $[\text{D}_3]\text{Ala}$ -labeled BP100 in DLPC. A)  $^{31}\text{P}$  NMR spectra before the  $^2\text{H}$  experiments at  $35^\circ\text{C}$ ; B)  $^2\text{H}$  NMR spectra at  $35^\circ\text{C}$ ; C)  $^2\text{H}$  NMR spectra at  $5^\circ\text{C}$ ; D)  $^{31}\text{P}$  NMR spectra after the  $^2\text{H}$  experiments at  $35^\circ\text{C}$ . The red bar indicates the estimated splitting for the label at position 8 at  $5^\circ\text{C}$ .

In DLPC, the  $^{15}\text{N}$  NMR spectra had shown a significantly tilted state at  $35^\circ\text{C}$ , which is confirmed by the  $^2\text{H}$  NMR data analysis, giving a helix tilt angle around  $60^\circ$  (between the helix axis and the bilayer normal) and an azimuthal angle of  $172^\circ$ . At  $5^\circ\text{C}$ , the  $^{15}\text{N}$  NMR spectra had indicated a transmembrane orientation, and the  $^2\text{H}$  NMR spectra indicated a tilt angle of about  $29^\circ$  and an azimuthal angle of  $164^\circ$ . This is not a perfectly upright orientation, but clearly, the peptide is much more tilted at lower temperatures.

In DLPC/lyso-LPC, the  $^{15}\text{N}$  NMR spectrum at  $35^\circ\text{C}$  had indicated a transmembrane state, with a  $^{15}\text{N}$  chemical shift similar to that found in DLPC at  $5^\circ\text{C}$ .  $^2\text{H}$  NMR analysis confirmed

these observations, giving a tilt angle of  $26^\circ$  and an azimuthal angle of  $165^\circ$  (as the difference compared to the orientation in DLPC at  $5^\circ\text{C}$  lies within the estimated error of the method). This comprehensive picture of helix (re-)orientations thus indicates that the lysolipids promote the transmembrane state, which is also favored by temperatures close to the lipid phase transition  $T_m$ . Lowering the temperature further to  $5^\circ\text{C}$  did not lead to much change in the  $^{15}\text{N}$  NMR chemical shift (Figure 3D), but the  $^2\text{H}$  NMR analysis suggests an even more inserted orientation of the peptide, with a tilt angle of  $7^\circ$ , indicating an essentially complete upright alignment in the bilayer. Yet, the fit was rather poor, with an RMSD of more than 6 kHz (the other fits

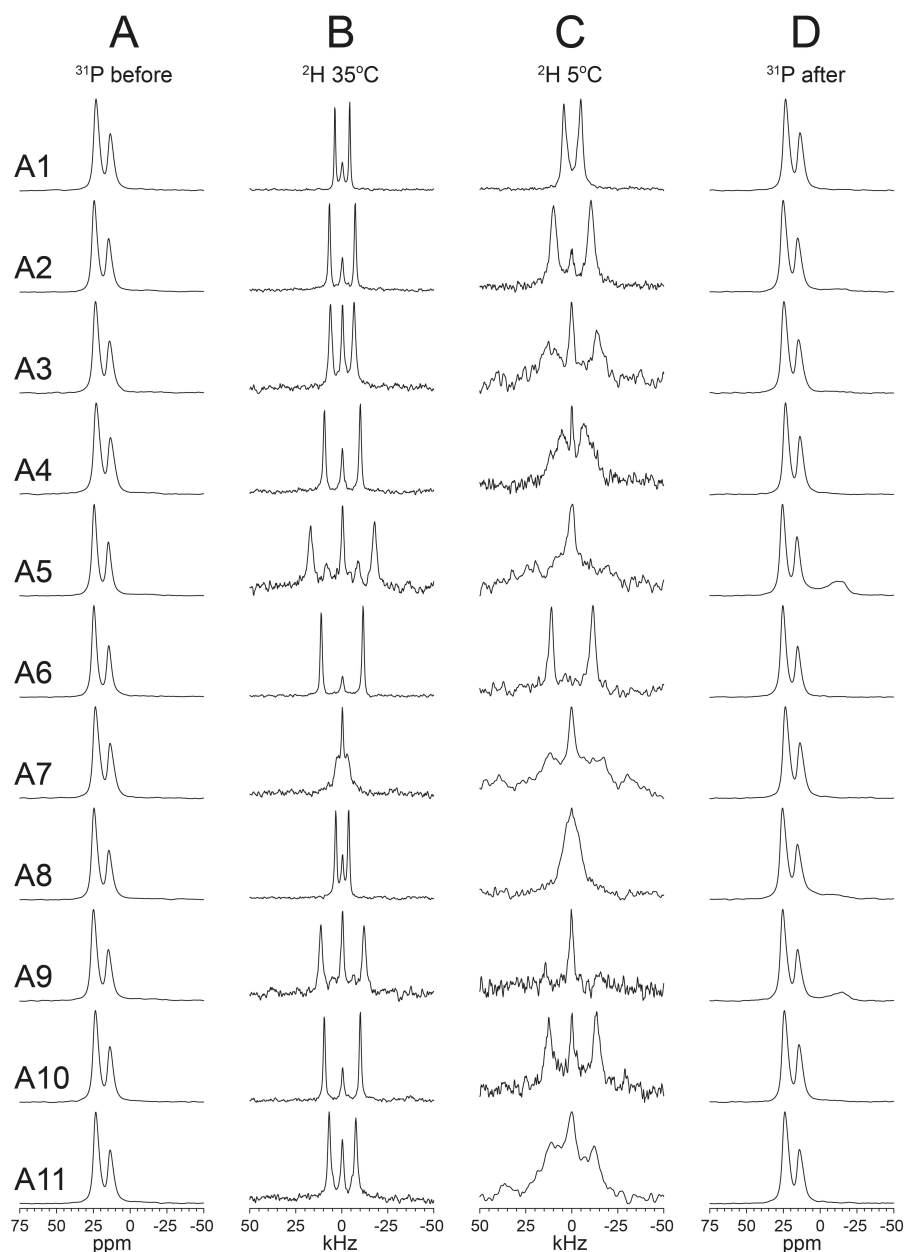


**Figure 6.**  $^2\text{H}$  NMR spectra of  $[\text{D}_3]\text{Ala}$ -labeled BP100 in DLPC/lyso-LPC (2:1). A)  $^{31}\text{P}$  NMR spectra before the  $^2\text{H}$  experiments at  $35^\circ\text{C}$ ; B)  $^2\text{H}$  NMR spectra at  $35^\circ\text{C}$ ; C)  $^2\text{H}$  NMR spectra at  $5^\circ\text{C}$ ; D)  $^{31}\text{P}$  NMR spectra after the  $^2\text{H}$  experiments at  $35^\circ\text{C}$ .

were good, with RMSDs below 3 kHz), so this result is not very reliable. Nonetheless, the helical wave (Figure 7H) looks significantly different compared to the one at  $35^\circ\text{C}$  (Figure 7F), and it is indeed similar to what would be expected for an upright peptide with a very small tilt angle. Therefore, it is plausible that BP100 is actually aligned almost perfectly upright in the membrane under these conditions.

### MD simulations

Molecular dynamics simulations were performed for BP100 in a DMPC lipid bilayer at 308 K. Two different starting positions of

the peptide were used in two separate simulations. In the first case, the peptide was inserted from the water phase and bound to the membrane surface. The simulation was then run for  $8\ \mu\text{s}$ , during which BP100 was always observed to remain more or less flat on the surface (S-state). This is called the S-state simulation and has been reported previously.<sup>[58]</sup> In the second simulation, to be reported here, the peptide was manually inserted into the lipid bilayer in a membrane-spanning orientation, with charged lysine side chains snorkeling to both sides. When the simulation was run, it was found that the peptide was stable in this inserted state (I-state) throughout the entire  $1\ \mu\text{s}$  simulation. Below, this is referred to as the I-state simulation.

**Table 2.**  $^2\text{H}$  NMR splittings [kHz] from experiments, at P/L = 1:20.<sup>[a]</sup>

| Peptide   | DLPC  |      | DLPC/lyso-LPC |      |
|-----------|-------|------|---------------|------|
|           | 35 °C | 5 °C | 35 °C         | 5 °C |
| BP100K1A  | 13.9  | 13.0 | 8.0           | 9.2  |
| BP100K2A  | 2.3   | 23.9 | 14.0          | 20.3 |
| BP100L3A  | 0     | 30.7 | 12.8          | 26.4 |
| BP100F4A  | 24.7  | 30.8 | 19.5          | 11.8 |
| BP100K5A  | 43.9  | 51.0 | 34.7          | 0    |
| BP100K6A  | 27.2  | 23.0 | 22.8          | 22.5 |
| BP100I7A  | 0     | 29.1 | 5.6           | 23.4 |
| BP100L8A  | 11.3  | 3.0  | 7.0           | 5.0  |
| BP100K9A  | 26.8  | 0    | 29.5          | 0    |
| BP100Y10A | 6.6   | 30.8 | 19.6          | 25.8 |
| BP100L11A | 2.0   | 29.7 | 14.5          | 23.4 |

[a] Only absolute values are available from experiments; therefore, no signs are given. The error in the splitting is estimated to  $\pm 2$  kHz.

**Table 3.** Best-fit orientation of BP100 in different bilayers, calculated from  $^2\text{H}$  NMR data.

| Lipid, T             | $\tau$ [°] | $\rho$ [°] | $\sigma_\tau$ [°] | $\sigma_\rho$ [°] | RMSD [kHz] |
|----------------------|------------|------------|-------------------|-------------------|------------|
| DLPC, 35 °C          | 58         | 172        | 36                | 16                | 2.8        |
| DLPC, 5 °C           | 29         | 164        | 19                | 0                 | 2.5        |
| DLPC/lyso-LPC, 35 °C | 26         | 165        | 36                | 21                | 2.4        |
| DLPC/lyso-LPC, 5 °C  | 7          | 200        | 6                 | 1                 | 6.6        |

In the S-state simulation, the peptide was initially fully helical. After 1.5  $\mu\text{s}$ , the N-terminal Lys1 and Lys2 became unfolded and remained so for the rest of the simulation, resulting in a reduction of helicity to approximately 80% and a significantly reduced tilt angle.<sup>[58]</sup> After that, refolding of the N terminus occurred only very rarely. The peptide was seen to be lying flat on the membrane surface throughout the entire simulation, as illustrated by the snapshot of Figure 8A. The most probable helix tilt angle was close to 90° (Figure 8C), with 10–20° fluctuations in the tilt angle. For symmetry reasons, the combination of  $\tau \approx 97^\circ$  and  $\rho \approx 351^\circ$  is equivalent to  $\tau \approx 83^\circ$  and  $\rho \approx 171^\circ$ .

In the I-state simulation, the peptide remained completely helical (except for Lys1), and it was much less mobile. The average helicity for each residue (the proportion of time points at which the residue is in a helical conformation, as defined in the Experimental Section) is plotted in Figure S11, showing that the peptide is fully helical for positions 3–11 in both simulations. In the I-state simulation (but not the S-state) also position 2 is fully helical, while the N-terminal Lys is not in a helical conformation in any simulation. A snapshot of the I-state simulation is shown in Figure 8B. The  $\tau$ - $\rho$  plot in Figure 8D shows the distribution of the orientational angles, with the most common orientation defined by  $\tau \approx 156^\circ$  and  $\rho \approx 117^\circ$  (equivalent to  $\tau \approx 24^\circ$  and  $\rho \approx 297^\circ$ ), corresponding to an almost upright peptide in the DMPC bilayer. Notably, numerous water molecules and phosphate groups are seen to be pulled rather deeply into the lipid bilayer from both sides by the snorkeling Lys side chains. The central ones tend to assume a rather stretched all-*trans* configuration.

The results of the MD simulations can be checked against the experimental  $^2\text{H}$  NMR data. From the simulation trajectories,

it is possible to calculate the hypothetical NMR splitting for any specific residue by analyzing the time-averaged orientation of the corresponding  $\text{C}_\alpha$ - $\text{C}_\beta$  bond vector with respect to the membrane normal. This is the splitting that would be measured in an NMR experiment if the residue were labeled with  $[\text{D}_3]\text{Ala}$  (assuming that the orientation of the  $\text{C}_\alpha$ - $\text{C}_\beta$  bond vector is not disturbed by labeling with a different side chain), so this prediction can be directly compared with the experimental values. The calculated splittings from the S-state simulation had been previously compared with  $^{19}\text{F}$  NMR data of BP100 in DMPC/DMPG,<sup>[22,58]</sup> even though only half of the positions could be labeled with  $^{19}\text{F}$ -Bpg in our first study.<sup>[22]</sup> In a later study, all 11 positions of BP100 were selectively labeled with  $[\text{D}_3]\text{Ala}$ , resulting in a complete set of  $^2\text{H}$  NMR data,<sup>[21]</sup> which makes it possible to compare the simulation with experiments in a more comprehensive way. Here, in Table 4, we give the calculated  $^2\text{H}$  NMR splittings for both S- and I-state simulations.

Figure 9 shows a fit of the back-calculated splittings, based on the same analysis method as previously used for the experimental NMR data.<sup>[21]</sup> For the S-state simulation, two periods are examined separately: 0–1.5  $\mu\text{s}$  with a higher helicity, and 1.5–8  $\mu\text{s}$  where the N terminus was unfolded. The change in conformation of the peptide after approximately 1.5  $\mu\text{s}$  of the simulation also leads to a change in the calculated splittings, as seen in Table 4, and a fit of the splitting also shows a change in tilt angle from 71° for the first 1.5  $\mu\text{s}$  to 86° in the 1.5–8  $\mu\text{s}$  time span (Figure 9, Table 5). The above fit of the experimental splittings gave a tilt angle of 76°, that is in between the two simulation values; the experimental fit also supported a fully folded helix over the entire length of the peptide.<sup>[21]</sup> This could

**Table 4.**  $^2\text{H}$  NMR splittings [kHz] from MD simulations (DMPC, P/L = 1:58).<sup>[a]</sup>

| Position | MD (S) 0–1.5 $\mu\text{s}$ | MD (S) 1.5–8 $\mu\text{s}$ | MD (I)           |
|----------|----------------------------|----------------------------|------------------|
| 1        | $-1.3 \pm 17.0$            | $+18.0 \pm 23.1$           | $-16.8 \pm 13.6$ |
| 2        | $+14.1 \pm 24.0$           | $+10.9 \pm 20.1$           | $-38.0 \pm 1.1$  |
| 3        | $-12.3 \pm 9.6$            | $+3.9 \pm 8.9$             | $-23.6 \pm 4.4$  |
| 4        | $-26.5 \pm 4.6$            | $-18.6 \pm 2.0$            | $+39.6 \pm 4.0$  |
| 5        | $+57.2 \pm 4.4$            | $+46.4 \pm 4.6$            | $-12.9 \pm 1.8$  |
| 6        | $-25.0 \pm 3.6$            | $-29.7 \pm 3.4$            | $-37.9 \pm 1.6$  |
| 7        | $+11.3 \pm 12.1$           | $+32.7 \pm 8.4$            | $-2.6 \pm 3.3$   |
| 8        | $-25.3 \pm 2.4$            | $-31.4 \pm 1.7$            | $+31.2 \pm 4.9$  |
| 9        | $+49.1 \pm 6.6$            | $+40.6 \pm 6.5$            | $-32.5 \pm 1.4$  |
| 10       | $-26.1 \pm 3.8$            | $-21.4 \pm 5.8$            | $-29.6 \pm 2.4$  |
| 11       | $-6.5 \pm 10.0$            | $+14.6 \pm 5.3$            | $+26.7 \pm 4.8$  |

[a] The sign of the splitting can be determined from the simulation and is therefore given here. The deviations are obtained from block averaging over the simulation trajectories.

**Table 5.** Best-fit orientations from  $^2\text{H}$  NMR splittings of BP100 in DMPC, back-calculated from MD simulations or determined from experiments.

|   | $\tau$ [°] | $\rho$ [°] | $\sigma_\tau$ [°] | $\sigma_\rho$ [°] | RMSD [kHz] |
|---|------------|------------|-------------------|-------------------|------------|
| MD S-state (0–1.5 $\mu\text{s}$ )           | 71         | 159        | 12                | 2                 | 3.9        |
| MD S-state (1.5–8 $\mu\text{s}$ )           | 86         | 156        | 0                 | 5                 | 4.2        |
| MD I-state                                  | 25         | 267        | 0                 | 4                 | 2.0        |
| $^2\text{H}$ NMR, P/L = 1:20 <sup>[a]</sup> | 76         | 168        | 21                | 23                | 3.7        |

[a] Values from experiments in DMPC/DMPG (3:1) at 35 °C.<sup>[21]</sup>

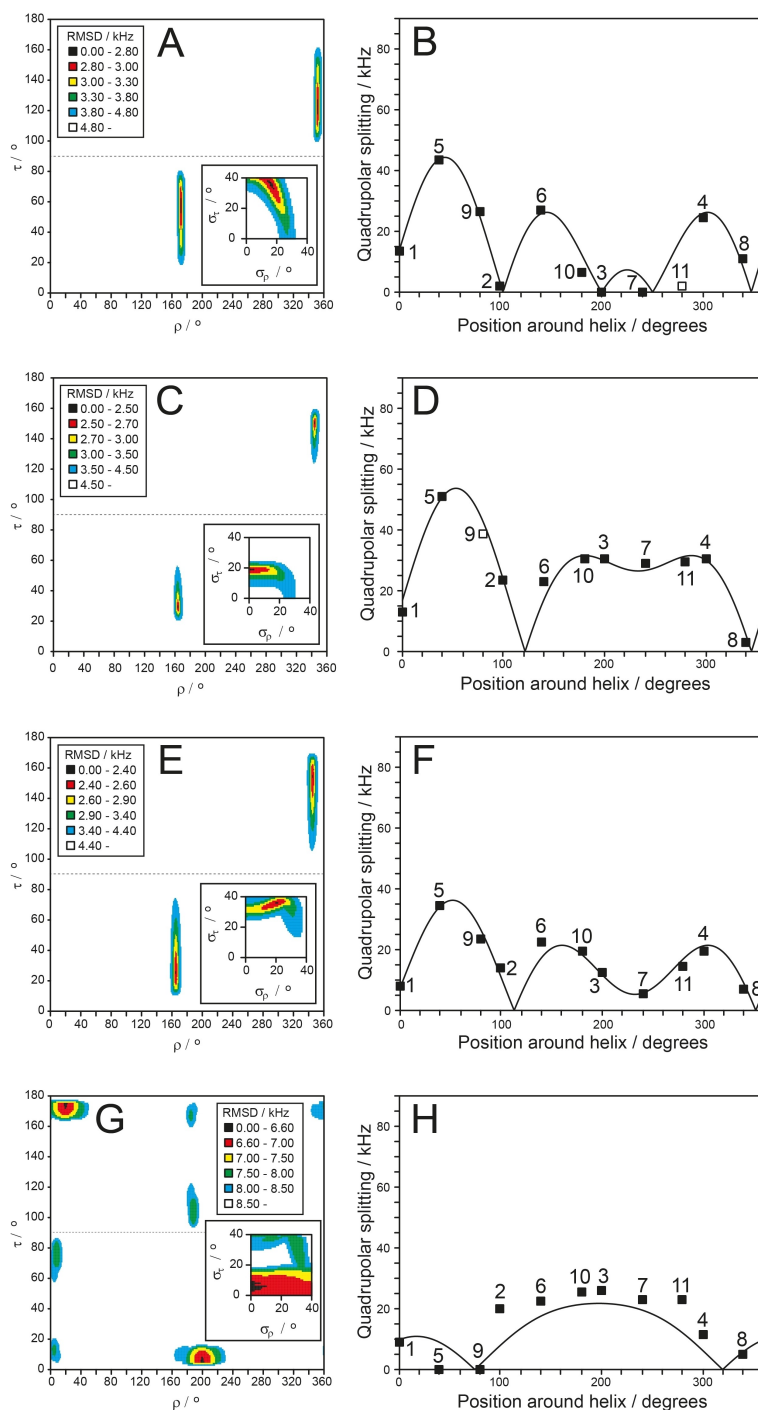


**Figure 7.** Analysis of  $^2\text{H}$  NMR data. A), B) BP100 in DLPC, P/L = 1:20 at 35 °C. A) The  $\tau$ - $\rho$  plot gives the RMSD between the experimental data and the helical waves that were systematically fitted to every combination of helix tilt angle  $\tau$  and rotation angle  $\rho$ , color-coded for the RMSD value at each point. The two minima at tilt angles of 58° and 122° are equivalent for symmetry reasons (i.e., peptides in either of the two monolayers, related by a 180° difference in  $\rho$ ). The best-fit value is  $\tau = 58^\circ, \rho = 172^\circ$ . The insert is a plot of RMSD for different values of the two parameters  $\sigma_\tau$  and  $\sigma_\rho$ , which reflect the range of whole-body fluctuations around the corresponding tilt and rotation angles. B) Helical wave of the best-fit solution. Experimental data are marked with squares, and the numbers indicate the labeled amino acid position in the sequence of BP100. All data points fit the curve well, except for position 11 (□), which was therefore excluded from the fit. C), D) are similar to (A) and (B), but using data from BP100 in DLPC at P/L = 1:20 and 5 °C. The best-fit orientation is  $\tau = 29^\circ, \rho = 164^\circ$ . The splitting from position 9 was ambiguous in the raw spectrum, and was therefore not used in the fit (□). E), F) show the data from BP100 in DLPC/lyso-LPC at P/L = 1:20 and 35 °C, with best-fit orientations of  $\tau = 26^\circ$  and  $\rho = 165^\circ$ . G), H) are similar to (A) and (B), but using data from BP100 in DLPC/lyso-LPC at P/L = 1:20 and 5 °C. The best-fit orientation is  $\tau = 7^\circ, \rho = 200^\circ$ , but the RMSD is in this case very high.

mean that BP100 is mostly in the fully folded state when observed during the first 1.5  $\mu\text{s}$  of the simulation, and it only

occasionally enters a less folded and more tilted state. There is a minor difference of about 10° in the rotation angle between

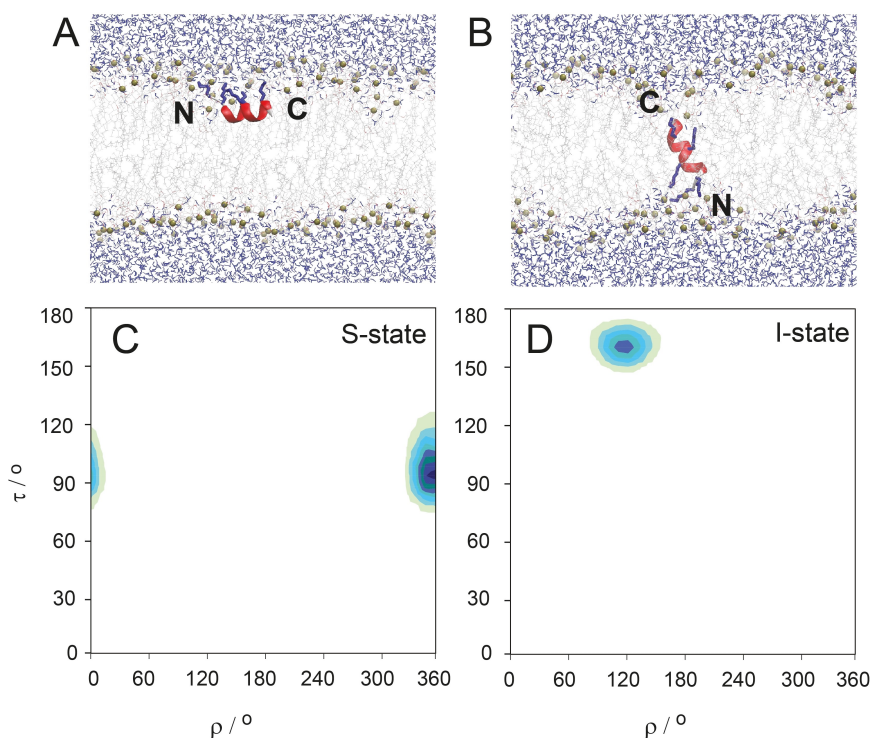


**Figure 8.** A) Snapshot of BP100 in the S-state simulation, showing a typical peptide orientation. Lipid phosphate groups are marked with golden spheres, lysine side chains are shown in dark blue. B) Snapshot of BP100 in the I-state simulation showing that the peptide can span the membrane as a stable monomer, with Lys side chains snorkeling towards either monolayer surface and thereby dragging water molecules (blue) into the membrane. C) Alignment of BP100 during the S-state simulation (for the time period of 1.5–8  $\mu$ s, after unfolding of the N terminus). The equilibrium orientation of BP100 is tilted  $97^\circ \pm 4^\circ$  (equivalent to  $83^\circ \pm 4^\circ$ ), and more strongly tilted helices up to  $120^\circ$  (i.e.,  $60^\circ$ ) can also be seen occasionally. D) Alignment of BP100 during the I-state simulation. The equilibrium orientation is tilted by  $156^\circ \pm 4^\circ$ , which is equivalent to  $24^\circ \pm 4^\circ$ .

the results of the simulation and experiments. Such (systematic) difference was previously reported for other helical peptides.<sup>[59]</sup>

For the I-state simulation, a tilt angle of  $25^\circ$  was observed, corresponding to an essentially upright alignment, that is a transmembrane orientation. For symmetry reasons the combination of  $\tau \approx 25^\circ$  and  $\rho \approx 267^\circ$  is equivalent to  $\tau \approx 155^\circ$  and  $\rho \approx 87^\circ$ . When this set of angles is compared with the orientation found from the  $^2\text{H}$  NMR experiments in DLPC at  $5^\circ\text{C}$ , the helix tilt is very similar, but the azimuthal angle is about  $100^\circ$  larger in the simulation. We note that in such a steep helix orientation (where  $\tau$  is close to  $0^\circ$  or  $180^\circ$ ), the corresponding value of  $\rho$  carries less structural meaning in terms of amphiphilicity than in a surface-bound helix, but it can nevertheless be determined experimentally with high confidence.

## Discussion

Membrane-active amphiphilic helices have been reported in many instances to take on different stable orientations in a membrane, reflecting their functional mechanism of permeabilization or translocation. The most obvious orientation for longitudinally amphiphilic helices is flat on the membrane surface, with the charged face pointing up toward the water, and hydrophobic side chains immersed more deeply in the hydrophobic interior of the bilayer. This surface-bound S-state

orientation has been described for virtually all amphipathic helices at low concentrations, and is also known to be the universally preferred state in lipid systems with negative spontaneous curvatures.<sup>[13]</sup> Another meaningful way to arrange amphiphilic helices is as a transmembrane orientation, where an oligometric assembly of peptides defines a water-filled pore across the membrane (with or without the participation of lipid head groups). In this case, the pore is lined by the charged faces of the helices, while the hydrophobic side chains point sideways and retain their contact with the lipid acyl chains. This inserted I-state has been observed for a limited number of amphipathic peptides so far, usually only under certain conditions. Systematic studies have revealed that the I-state tends to be favored by 1) lipids with positive spontaneous curvatures (e.g., lysolipids),<sup>[13,17,18,56]</sup> 2) high peptide concentration,<sup>[18,45,54]</sup> 3) long peptides (long enough to span the membrane),<sup>[15,17]</sup> 4) peptides with one charged and one hydrophobic terminus,<sup>[16]</sup> and 5) in special cases by peptide-peptide interactions (one example being the PGLa/magainin 2 synergistic pair of peptides).<sup>[60–63]</sup>

In the above-mentioned studies, the peptides were usually around 20 amino acids long, which is a perfect size to span a typical lipid bilayer. Far less is known about the behavior of shorter peptides like BP100, and it is certainly not justified to assume that they should follow the same rules and undergo the same kinds of structural rearrangements. That is because short

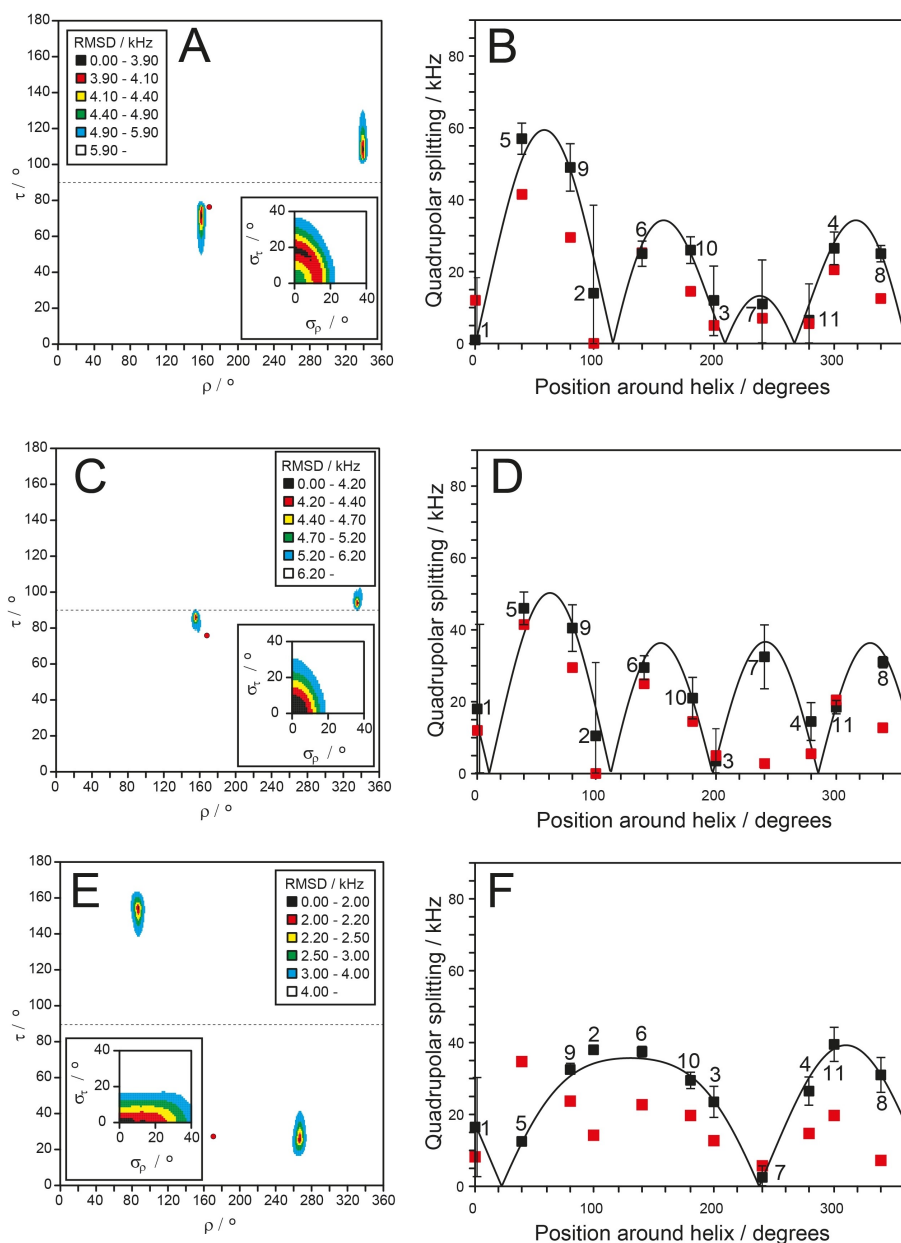


**Figure 9.** A), B) Analysis of splittings back-calculated from the S-state simulation, from 0 to 1.5  $\mu$ s. A) Plot of the RMSD between the fitted data and the helical wave for different values of tilt angle  $\tau$  and rotation angle  $\rho$ , color coded for the value at each point. The two minima at tilt angles of  $71^\circ$  and  $109^\circ$  are equivalent for symmetry reasons, as they correspond to peptides in the two bilayer leaflets. The best-fit value from the experimental data ( $\tau = 86^\circ$ ,  $\rho = 168^\circ$ ) is marked  $\bullet$ . The insert is a plot of the RMSD for different values of the dynamical parameters  $\sigma_\tau$  and  $\sigma_\rho$ . B) Helical wave of the best-fit solution fitted to the back-calculated quadrupolar couplings of all residues averaged over the MD simulations ( $\bullet$ ) and compared to the experimental  $^2\text{H}$  NMR data ( $\circ$ ) of BP100 in DMPC/DMPG (3:1) bilayers at P/L = 1:20.<sup>[21]</sup> The black curves show the best fit to a helical wave of the MD data. C), D) are similar to (A) and (B) but using splittings from the S-state simulation from 1.5 to 8  $\mu$ s. The best-fit orientation is  $\tau = 86^\circ$ ,  $\rho = 156^\circ$ . E), F) are similar to (A) and (B) but using splittings from the I-state simulation. The experimental  $^2\text{H}$  NMR data ( $\circ$ ) in (F) were collected in DLPC/lyso-LPC at  $35^\circ\text{C}$ . The best-fit orientation is  $\tau = 25^\circ$ ,  $\rho = 267^\circ$ . The best-fit orientation from the experimental data is marked  $\bullet$ . Error bars are given for simulated values. Some error bars are smaller than the size of the symbols. For experimental values, the error is estimated to be 2 kHz.

peptides tend to be more mobile, have a more flexible conformation, and they are too short to span a membrane. BP100 is highly charged (+6) and indeed very short with its 11 amino acids, although it forms a proper amphipathic  $\alpha$ -helix when bound to a lipid bilayer. Several structural studies have been previously devoted to BP100 and its interactions with lipid membranes. So far, this helical peptide has always been found

to reside on the bilayer surface under a wide range of tested conditions,<sup>[21,30]</sup> even under conditions where other peptides – such as MSI-103 and PGLa – change their orientation.<sup>[17,54]</sup> It seemed plausible indeed that the short 11-mer BP100 was far less likely to insert into a membrane compared to those longer peptides (with about 21 amino acids), because its length of about  $16.5 \text{ \AA}$  is simply too short to span the membrane. The

hydrophobic thickness of DMPC at 30 °C (in the liquid crystalline phase) is close to 25.4 Å, and that of thinner DLPC membranes is 20.9 Å.<sup>[64]</sup> The thickness tends to increase slightly upon lowering the temperature,<sup>[65]</sup> and in the gel phase every lipid bilayer becomes much thicker due to the dramatic increase in acyl chain order; for example, DMPC at 10 °C has a hydrophobic thickness of 30 Å.<sup>[66]</sup>

It has been reported that peptides can induce local membrane thinning, which has been proposed as a possible functional effect of BP100.<sup>[67]</sup> Furthermore, solid-state NMR studies have shown that in the presence of BP100 at P/L = 1:25, the order parameters of deuterated lipid chains was reduced by up to 30 %, which indicates significant membrane thinning.<sup>[30]</sup> In those papers the thinning effect was not quantified, but values have been published for other membrane-bound peptides. For example, when the short WALP16 transmembrane model helix (length 24 Å assuming an ideal helix) was inserted into a thick di-18:0-PC (DSPC) bilayer (hydrophobic thickness 28.5 Å) at P/L = 1:30, a thinning of 0.4 Å was noticed.<sup>[68]</sup> For melittin in di-20:1-PC bilayers at P/L = 1:50 or higher, a thinning of 4 % was reported.<sup>[65,69]</sup> These effects are quite small, so even for a thin DLPC bilayer, a thinning in this range would mean that the membrane is still too thick for BP100 to span it. However, the addition of lysolipids to the bilayer will make it even thinner, because there is less volume of the acyl chains while a similar headgroup area is maintained. We have not found any experimental data about how much thinner membranes get in the presence of a high amount of lysolipids. For a very crude estimate, we note that for a 2:1 mixture of for example DLPC and lyso-LPC, there is 5/6 the number of acyl chains compared to pure DLPC. If the headgroup area stays constant, then the bilayer thickness would be reduced to  $(5/6) \times 20.9 \text{ Å} = 17.4 \text{ Å}$ . Including some additional thinning effect from the peptide, it is then possible that BP100 would just about be able to span the membrane. This line of arguments may be the underlying reason why we observe the inserted state even at high temperature in the presence of lysolipids.

Another point that had been initially assumed not to support an insertion of BP100 rested on the finding that the short and essentially egg-shaped peptide body was extremely mobile, and therefore should be less likely to self-assemble into active pores because of these high dynamics.<sup>[21,22]</sup> We can furthermore note that the NMR data gives information on the orientation of the helix in the membrane, but not about the oligomeric state of the peptide. Large oligomers are expected to be less mobile, so the high dynamics found in the NMR analysis is an argument against large oligomers, while small oligomers such as dimers cannot be excluded.

In this study we used a powerful combination of solid-state NMR methods to investigate a wider range of conditions than before, and to study the orientation of BP100 in increasing detail: 1) Highly sensitive <sup>19</sup>F NMR spectroscopy was applied to scan numerous conditions to find conditions where BP100 actually changed its spectral pattern, reflecting a qualitative change in orientation and/or dynamics. 2) <sup>15</sup>N NMR spectroscopy was carried out on peptides with a single <sup>15</sup>N-label to obtain an approximate helix tilt angle and thereby show for the

first time that BP100 was actually inserted in a transmembrane alignment. 3) <sup>2</sup>H NMR spectroscopy was finally used to obtain an accurate structural description of this I-state in terms of helix tilt and azimuthal rotation angle, including an estimate of whole-body fluctuations. An overview of these orientations found under different conditions is schematically illustrated in Figure 10.

It was thus possible to conclusively show that BP100 can assume a stable transmembrane orientation in thin DLPC membranes [with a hydrophobic thickness of 20.9 Å<sup>[64]</sup>] at temperatures close to the gel-to-liquid crystalline phase transition ( $T_m$ ), even at quite a low concentration (P/L = 1:100). Even in DMPC (with a hydrophobic thickness of 25.4 Å<sup>[64]</sup>) at high concentrations (P/L = 1:20), slightly above the  $T_m$ , BP100 is in a highly tilted and possibly even transmembrane state according to <sup>15</sup>N NMR spectra. This finding was unexpected, since the membrane is much thicker than the length of an ideal helix of 11 amino acids (1.5 Å per residue leads to a helix length of only 16.5 Å). However, an indication of how this alignment may be possible, came from MD simulations.

Two simulations were performed for BP100 in DMPC bilayers at 35 °C. In one, the peptide was first located in water and allowed to bind to the membrane, where it stayed on the surface, in an S-state. In the other simulation, the peptide initially spanned the membrane in an inserted I-state, where

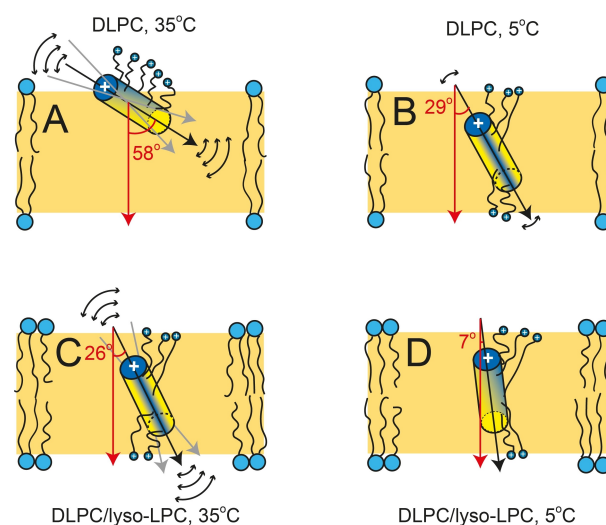


**Figure 10.** Summary of the orientation of BP100 as determined from <sup>2</sup>H NMR data analysis. The peptide is illustrated as a cylinder with blue (polar) and yellow (hydrophobic) faces, and the helix axis is defined as pointing from the N to the C terminus. Curved arrows indicate dynamics. Charged Lys side chains are shown schematically with possible snorkeling according to simulations. Only one peptide is shown (as we cannot tell from these NMR data whether oligomers are formed). The hydrophobic part of the membrane is shown in orange; for simplicity lipids are only shown at the edges and any putative local membrane thinning by the peptide is not indicated. The tilt angle with respect to the membrane normal (red arrow) is shown in each case. A) In DLPC bilayers at 35 °C, BP100 is slightly tilted on the membrane surface and has a high mobility. B) In DLPC bilayers at 5 °C, the helix is inserted in the membrane and has a lower mobility. C) In DLPC/lyso-LPC (2:1) bilayers at 35 °C, the peptide is inserted in the membrane and has a high mobility. D) In DLPC/lyso-LPC (2:1) bilayers at 5 °C, it is inserted in the membrane in an almost upright position and is almost completely immobilized.

the snorkeling Lys side chains stretched out to reach the polar face of the bilayer on both sides. In the S-state simulation, the peptide was seen to be very mobile, and it showed a considerable variation in its tilt angle during the simulation. However, the helix mostly remained flat on the membrane surface and never reached an inserted I-state. In the I-state simulation, which started off with a transmembrane orientation, this alignment remained stable during the entire 1  $\mu$ s simulation. There was only some minor variation in the tilt angle, but the peptide never flipped into the S-state. These findings suggest that snorkeling side chains may indeed support an I-state of BP100, even at high temperatures in quite thick DMPC membranes. It thus seems that both orientations are possible for BP100, but there is a large energetic barrier to go from one to the other. It is hard to observe any transitions between the states using MD simulations with simulation times of 10  $\mu$ s at best.

Even if the I-state simulations show that a transmembrane orientation of a single, monomeric BP100 peptide is stable on a 1  $\mu$ s time scale, it is unlikely that this scenario is found in a real membrane. Even if snorkeling is energetically relatively cheap,<sup>[70]</sup> a flip from the surface into the transmembrane state would need to overcome a relatively high energy barrier of translocating some of the charged side chains across the bilayer core. The NMR experiments clearly showed that the I-state occurs only at high peptide concentrations, indicating that insertion is a cooperative process, wherein a peptide complex is formed. Additionally, even if the tilt angle in the I-state simulation is similar to that found in DLPC at 5 °C using <sup>2</sup>H NMR spectroscopy, the rotation angle deviated strongly from experiment. This difference may well be attributed to peptide-peptide interactions that are involved in the transmembrane state that is observed by experiments, but which are missing in the MD simulation of a single peptide.

<sup>2</sup>H NMR experiments under the simulated conditions (low concentration in DMPC) show a surface orientation, fitting well with the result of the S-state simulation. Yet, an equilibrium seems to prevail. While BP100 is aligned almost completely on the surface of DMPC at 35 °C, with increasing concentration and upon lowering the temperature to slightly above the  $T_m$ , the transmembrane orientation becomes more favorable. At even lower temperatures in the gel phase, which is significantly thicker than the fluid phase, the surface state is observed again.

One reason for this behavior could be that at high concentrations and low temperatures, dynamics are reduced, and peptide-peptide interactions become stronger, which could favor the transmembrane complex. In the gel phase, there is even lower dynamics, but the acyl chains are stretched and the membrane becomes thicker, so that BP100 is again pushed out of the membrane and re-locates to the surface. Another possible explanation for the inserted state could be that the membrane close to the  $T_m$  forms some gel-phase domains and some liquid-crystalline domains. In each of these domains, BP100 is most favored on the membrane surface, but in the defects between the domains, the peptides might find conditions favoring a transmembrane orientation. At the actual phase transition temperature  $T_m$ , the maximal number of

domain boundaries is available, and here, BP100 is found almost exclusively in a transmembrane orientation.

Notably, in membranes containing lyso-PC, the transmembrane orientation is also found at temperatures well above the  $T_m$ . This indicates that gel phase domains and defects between domains are not necessary for insertion. Instead, it is clear that lysolipids have a strong positive spontaneous curvature due to their molecular shape with a large headgroup and only a single acyl chain, whereas DMPC and DLPC, with two acyl chains each, have only a small positive spontaneous curvature. We recently showed for the longer amphiphilic helix MSI-103 that stable transmembrane pores are formed in bilayers containing lysolipids. It was demonstrated that these pores are enriched in lysolipids, which are most likely also lining the toroidal wormhole type pores.<sup>[18]</sup> As the temperature is lowered, the acyl chains tend to stretch and get longer, leading to a smaller cross-section, giving DMPC and DLPC a higher positive spontaneous curvature. This process also increases the hydrophobic thickness of the membrane at the same time, but if the peptides are already arranged on the curved inside of the wormhole, this might not be a problem. This structural model can thus explain both, the insertion of BP100 in DMPC or DLPC close to their respective  $T_m$ , as well as the insertion in the presence of lysolipids even at high temperatures. With this toroidal wormhole model, the peptide length should not be as important as in a barrel stave. However, we did find that BP100 gets more easily inserted into DLPC than into DMPC, so there seems to be some effect of membrane thickness in relation to peptide length. When using a suitably thin membrane, we postulate that it should be possible to eventually flip any amphipathic helix of any length into an inserted state, either by setting the temperature close to the  $T_m$ , or by adding some lysolipids, provided that the peptide concentration is sufficiently high. An obvious limitation of the present study is that we have only studied a single short peptide. To be able to generalize and propose more robust conclusions, it will be important to study and compare also other short peptides using the same range of methods, and for example investigate the influence of charge, hydrophobicity, and other properties on the orientation of short amphiphilic helices in membranes.

Peptide orientation is known to be strongly dependent on membrane properties. Therefore, the fact that conditions can be found where a peptide has a stable transmembrane orientation does not mean that this must also be the case under biologically relevant conditions, which have to deal with highly transient events anyhow. It is rather the other way around, that is, once there are indications that the biological activity is related to peptides in a surface orientation or a transmembrane orientation, then a suitable model membrane system can be found where the desired peptide orientation will dominate. In other words, our ability to trap a normally short-lived, transient state simply by using the appropriate kinds of lipids, is very useful, as it allows us to study the peptide in this particular state using biophysical methods under stable conditions. We therefore hope that the present study will increase the range of suitable model membrane conditions with well-

characterized properties, and thereby help to make better choices of model systems for future biophysical studies.

## Conclusions

The orientation of BP100 in membranes was investigated under a wide range of conditions by using oriented CD and solid-state NMR methods.  $^{19}\text{F}$  NMR spectroscopy has a very high sensitivity and was used to screen conditions to detect a structural rearrangement of BP100. Subsequent  $^{15}\text{N}$  NMR studies under those conditions showed that BP100 was in a transmembrane-inserted state, and  $^2\text{H}$  NMR spectroscopy was used to characterize this orientation with high accuracy (Figure 10). It might seem quite unexpected that this short undecamer peptide, which was previously only ever found on the membrane surface, can in fact assume a stable transmembrane orientation. However, our interpretation of extended (snorkeling) Lys side chains, as found in a MD simulation, provides a plausible explanation for such a stable state. These results suggest that it should be possible to find special conditions for virtually any amphipathic peptide, under which it can be placed flat onto the membrane surface or flipped into an upright transmembrane state. This versatility in manipulating the peptide-lipid interactions will also be useful for future biophysical studies of many other peptides.

## Acknowledgements

We thank Andrea Eisele and Kerstin Scheubeck for helping with peptide synthesis, Dr. Stephan Grage and Markus Schmitt for their support with NMR hardware, and Bianca Posselt and Siegmund Roth for their CD support. We thank the LIPPSO group at the Chemistry Department, University of Girona, and the CIDSAV group at the Laboratory of Plant Pathology, Institute of Food and Agricultural Technology-CIDSAV-XaRTA, University of Girona for their support. We acknowledge financial support for NMR hardware from the German Research Foundation (DFG) project "INST 121384/58-1 FUGG". This work was also supported financially by the Helmholtz Association Program BIF-TM, by the DFG grant UL127/7-1, by the DAAD "Portugal-Ações Integradas Luso-Alemãs/DAAD-GRICES" grant D/07/13644, and by the Fundação para a Ciência e a Tecnologia grant SFRH/BD/24778/2005. Open Access funding enabled and organized by Projekt DEAL.

## Conflict of Interest

The authors declare no conflict of interest.

## Data Availability Statement

The data that support the findings of this study are available in the supplementary material of this article.

**Keywords:** antimicrobials · cationic amphipathic alpha-helices · cell-penetrating mechanisms · circular dichroism · peptide alignment in oriented bilayers · side-chain snorkeling

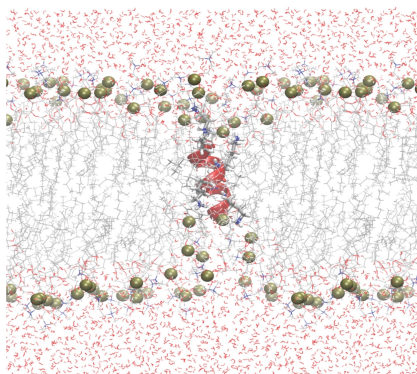
- [1] M.-A. Sani, F. Separovic, *Acc. Chem. Res.* **2016**, *49*, 1130–1138.
- [2] W. C. Wimley, *ACS Chem. Biol.* **2010**, *5*, 905–917.
- [3] K. A. Brogden, *Nat. Rev. Microbiol.* **2005**, *3*, 238–250.
- [4] L. T. Nguyen, E. F. Haney, H. J. Vogel, *Trends Biotechnol.* **2011**, *29*, 464–472.
- [5] M. Magana, M. Pushpanathan, A. L. Santos, L. Leanse, M. Fernandez, A. Ioannidis, M. A. Giulianotti, Y. Apidianakis, S. Bradfute, A. L. Ferguson, A. Cherkasov, M. N. Selem, C. Pinilla, C. de la Fuente-Nunez, T. Lazaridis, T. Dai, R. A. Houghton, R. E. W. Hancock, G. P. Tegos, *Lancet Infect. Dis.* **2020**, *20*, e216–e230.
- [6] P. Wadhvani, P. Tremouilhac, E. Strandberg, S. Afonin, S. L. Grage, M. Ieronimo, M. Berditsch, A. S. Ulrich, *Current Fluoroorganic Chemistry: New Synthetic Directions, Technologies, Materials, and Biological Applications* (Eds.: V. A. Soloshonok, K. Mikami, T. Yamazaki, J. T. Welch, J. F. Honek), American Chemical Society, Washington DC **2007**, pp. 431–446.
- [7] A. S. Ulrich, P. Wadhvani, U. H. N. Dürr, S. Afonin, R. W. Glaser, E. Strandberg, P. Tremouilhac, C. Sachse, M. Berditschevskaia, S. L. Grage, *NMR Spectroscopy of Biological Solids* (Ed.: A. Ramamoorthy), CRC Press, Boca Raton **2006**, pp. 215–236.
- [8] E. Strandberg, A. S. Ulrich, *Concepts Magn. Reson. Part A* **2004**, *23* A, 89–120.
- [9] E. Strandberg, A. S. Ulrich, *Modern Magnetic Resonance*, 2nd ed. (Ed.: G. A. Webb), Springer International, Cham **2017**, pp. 1–13.
- [10] J. Bürck, P. Wadhvani, S. Fanghänel, A. S. Ulrich, *Acc. Chem. Res.* **2016**, *49*, 184–192.
- [11] Y. Wu, H. W. Huang, G. A. Olah, *Biophys. J.* **1990**, *57*, 797–806.
- [12] J. Zerweck, E. Strandberg, J. Bürck, J. Reichert, P. Wadhvani, O. Kukhareenko, A. S. Ulrich, *Eur. Biophys. J.* **2016**, *45*, 535–547.
- [13] E. Strandberg, A. S. Ulrich, *Biochim. Biophys. Acta* **2015**, *1848*, 1944–1954.
- [14] W. L. Maloy, U. P. Kari, *Biopolymers* **1995**, *37*, 105–122.
- [15] A. Grau-Campistany, E. Strandberg, P. Wadhvani, J. Reichert, J. Bürck, F. Rabanal, A. S. Ulrich, *Sci. Rep.* **2015**, *5*, 9388.
- [16] E. Strandberg, D. Bentz, P. Wadhvani, J. Bürck, A. S. Ulrich, *Biochim. Biophys. Acta* **2020**, *1862*, 183243.
- [17] A. Grau-Campistany, E. Strandberg, P. Wadhvani, F. Rabanal, A. S. Ulrich, *J. Phys. Chem. Lett.* **2016**, *7*, 1116–1120.
- [18] E. Strandberg, D. Bentz, P. Wadhvani, A. S. Ulrich, *Sci. Rep.* **2020**, *10*, 4710.
- [19] E. Badosa, R. Ferre, M. Planas, L. Feliu, E. Besalu, J. Cabrefiga, E. Bardaji, E. Montesinos, *Peptides* **2007**, *28*, 2276–2285.
- [20] R. Ferre, M. N. Melo, A. D. Correia, L. Feliu, E. Bardaji, M. Planas, M. Castanho, *Biophys. J.* **2009**, *96*, 1815–1827.
- [21] H. Zamora-Carreras, E. Strandberg, P. Mühlhäuser, J. Bürck, P. Wadhvani, M. Á. Jiménez, M. Bruix, A. S. Ulrich, *Biochim. Biophys. Acta* **2016**, *1858*, 1328–1338.
- [22] P. Wadhvani, E. Strandberg, J. van den Berg, C. Mink, J. Bürck, R. Ciriello, A. S. Ulrich, *Biochim. Biophys. Acta* **2014**, *1838*, 940–949.
- [23] K. Eggenberger, C. Mink, P. Wadhvani, A. S. Ulrich, P. Nick, *ChemBioChem* **2011**, *12*, 132–137.
- [24] C. Mink, E. Strandberg, P. Wadhvani, M. N. Melo, J. Reichert, I. Wacker, M. A. R. B. Castanho, A. S. Ulrich, *Front. Cell. Infect. Microbiol.* **2021**, *11*.
- [25] G. B. Fields, R. L. Noble, *Int. J. Pept. Protein Res.* **1990**, *35*, 161–214.
- [26] P. Wadhvani, R. F. Epand, N. Heidenreich, J. Bürck, A. S. Ulrich, R. M. Epand, *Biophys. J.* **2012**, *103*, 265–274.
- [27] C. N. Pace, F. Vajdos, L. Fee, G. Grimsley, T. Gray, *Protein Sci.* **1995**, *4*, 2411–2423.
- [28] J. Bürck, S. Roth, P. Wadhvani, S. Afonin, N. Kanithasen, E. Strandberg, A. S. Ulrich, *Biophys. J.* **2008**, *95*, 3872–3881.
- [29] L. Greenspan, *J. Res. Natl. Bur. Stand. Sect. A* **1977**, *81*, 89–96.
- [30] J. Misiewicz, S. Afonin, S. L. Grage, J. van den Berg, E. Strandberg, P. Wadhvani, A. S. Ulrich, *J. Biomol. NMR* **2015**, *61*, 287–298.
- [31] J. P. Ulmschneider, J. C. Smith, M. B. Ulmschneider, A. S. Ulrich, E. Strandberg, *Biophys. J.* **2012**, *103*, 472–482.
- [32] S. Afonin, P. K. Mikhailiuk, I. V. Komarov, A. S. Ulrich, *J. Pept. Sci.* **2007**, *13*, 614–623.
- [33] P. K. Mikhailiuk, S. Afonin, A. N. Chernega, E. B. Rusanov, M. O. Platonov, G. G. Dubinina, M. Berditsch, A. S. Ulrich, I. V. Komarov, *Angew. Chem. Int. Ed.* **2006**, *45*, 5659–5661; *Angew. Chem.* **2006**, *118*, 5787–5789.

- [34] S. Reisser, S. Prock, H. Heinzmann, A. S. Ulrich, *Biochem. Mol. Biol. Educ.* **2018**, *46*, 403–409.
- [35] S. L. Grage, S. Afonin, A. S. Ulrich, *Antimicrobial Peptides. Methods and Protocols, Vol. 618* (Eds.: A. Giuliani, A. C. Rinaldi), Humana, Totowa **2010**, pp. 183–209.
- [36] H. W. Huang, Y. Wu, *Biophys. J.* **1991**, *60*, 1079–1087.
- [37] L. Yang, T. A. Harroun, T. M. Weiss, L. Ding, H. W. Huang, *Biophys. J.* **2001**, *81*, 1475–1485.
- [38] W. T. Heller, A. J. Waring, R. I. Lehrer, H. W. Huang, *Biochemistry* **1998**, *37*, 17331–17338.
- [39] S. Fanghänel, P. Wadhvani, E. Strandberg, W. P. R. Verdurmen, J. Bürck, S. Ehni, P. K. Mykhailiuk, S. Afonin, D. Gerthsen, I. V. Komarov, R. Brock, A. S. Ulrich, *PLoS One* **2014**, *9*, e99653.
- [40] P. Wadhvani, J. Reichert, E. Strandberg, J. Bürck, J. Misiewicz, S. Afonin, N. Heidenreich, S. Fanghänel, P. K. Mykhailiuk, I. V. Komarov, A. S. Ulrich, *Phys. Chem. Chem. Phys.* **2013**, *15*, 8962–8971.
- [41] K. Koch, S. Afonin, M. Ieronimo, M. Berditsch, A. S. Ulrich, *Top. Curr. Chem.* **2012**, *306*, 89–118.
- [42] P. Wadhvani, E. Strandberg, N. Heidenreich, J. Bürck, S. Fanghänel, A. S. Ulrich, *J. Am. Chem. Soc.* **2012**, *134*, 6512–6515.
- [43] M. Ieronimo, S. Afonin, K. Koch, M. Berditsch, P. Wadhvani, A. S. Ulrich, *J. Am. Chem. Soc.* **2010**, *132*, 8822–8824.
- [44] D. Maisch, P. Wadhvani, S. Afonin, C. Böttcher, B. Koksche, A. S. Ulrich, *J. Am. Chem. Soc.* **2009**, *131*, 15596–15597.
- [45] S. Afonin, U. H. N. Dürr, P. Wadhvani, J. B. Salgado, A. S. Ulrich, *Top. Curr. Chem.* **2008**, *273*, 139–154.
- [46] S. Afonin, S. L. Grage, M. Ieronimo, P. Wadhvani, A. S. Ulrich, *J. Am. Chem. Soc.* **2008**, *130*, 16512–16514.
- [47] E. Strandberg, N. Kanithasen, J. Bürck, P. Wadhvani, D. Tiltak, O. Zwerneemann, A. S. Ulrich, *Biochemistry* **2008**, *47*, 2601–2616.
- [48] P. Wadhvani, J. Bürck, E. Strandberg, C. Mink, S. Afonin, A. S. Ulrich, *J. Am. Chem. Soc.* **2008**, *130*, 16515–16517.
- [49] S. L. Grage, A. V. Suleymanova, S. Afonin, P. Wadhvani, A. S. Ulrich, *J. Magn. Reson.* **2006**, *183*, 77–86.
- [50] E. Strandberg, P. Wadhvani, P. Tremouilhac, U. H. N. Dürr, A. S. Ulrich, *Biophys. J.* **2006**, *90*, 1676–1686.
- [51] R. W. Glaser, C. Sachse, U. H. N. Dürr, S. Afonin, P. Wadhvani, E. Strandberg, A. S. Ulrich, *Biophys. J.* **2005**, *88*, 3392–3397.
- [52] S. Afonin, U. H. N. Dürr, R. W. Glaser, A. S. Ulrich, *Magn. Reson. Chem.* **2004**, *42*, 195–203.
- [53] R. W. Glaser, C. Sachse, U. H. N. Dürr, P. Wadhvani, A. S. Ulrich, *J. Magn. Reson.* **2004**, *168*, 153–163.
- [54] P. Tremouilhac, E. Strandberg, P. Wadhvani, A. S. Ulrich, *Biochim. Biophys. Acta* **2006**, *1758*, 1330–1342.
- [55] E. Strandberg, F. Schweigardt, P. Wadhvani, J. Bürck, J. Reichert, H. L. P. Cravo, L. Burger, A. S. Ulrich, *Sci. Rep.* **2020**, *10*, 12300.
- [56] E. Strandberg, J. Zerweck, P. Wadhvani, A. S. Ulrich, *Biophys. J.* **2013**, *104*, L9–11.
- [57] E. Strandberg, D. Tiltak, S. Ehni, P. Wadhvani, A. S. Ulrich, *Biochim. Biophys. Acta* **2012**, *1818*, 1764–1776.
- [58] Y. Wang, T. Zhao, D. Wei, E. Strandberg, A. S. Ulrich, J. P. Ulmschneider, *Biochim. Biophys. Acta* **2014**, *1838*, 2280–2288.
- [59] S. Reisser, E. Strandberg, T. Steinbrecher, M. Elstner, A. S. Ulrich, *J. Chem. Theory Comput.* **2018**, *14*, 6002–6014.
- [60] E. Strandberg, P. Tremouilhac, P. Wadhvani, A. S. Ulrich, *Biochim. Biophys. Acta* **2009**, *1788*, 1667–1679.
- [61] P. Tremouilhac, E. Strandberg, P. Wadhvani, A. S. Ulrich, *J. Biol. Chem.* **2006**, *281*, 32089–32094.
- [62] E. S. Salnikov, B. Bechinger, *Biophys. J.* **2011**, *100*, 1473–1480.
- [63] J. Zerweck, E. Strandberg, O. Kukharensko, J. Reichert, J. Burck, P. Wadhvani, A. S. Ulrich, *Sci. Rep.* **2017**, *7*, 13153.
- [64] N. Kucerka, Y. Liu, N. Chu, H. I. Petrache, S. Tristram-Nagle, J. F. Nagle, *Biophys. J.* **2005**, *88*, 2626–2637.
- [65] C. J. Su, M. T. Lee, K. F. Liao, O. Shih, U. S. Jeng, *Phys. Chem. Chem. Phys.* **2018**, *20*, 26830–26836.
- [66] S. Tristram-Nagle, Y. F. Liu, J. Legleiter, J. F. Nagle, *Biophys. J.* **2002**, *83*, 3324–3335.
- [67] M. C. Manzini, K. R. Perez, K. A. Riske, J. C. Bozelli Jr., T. L. Santos, M. A. da Silva, G. K. Saraiva, M. J. Politi, A. P. Valente, F. C. Almeida, H. Chaimovich, M. A. Rodrigues, M. P. Bemquerer, S. Schreier, I. M. Cuccovia, *Biochim. Biophys. Acta* **2014**, *1838*, 1985–1999.
- [68] M. R. de Planque, D. V. Greathouse, R. E. Koeppe II, H. Schafer, D. Marsh, J. A. Killian, *Biochemistry* **1998**, *37*, 9333–9345.
- [69] C. J. Su, S. S. Wu, U. S. Jeng, M. T. Lee, A. C. Su, K. F. Liao, W. Y. Lin, Y. S. Huang, C. Y. Chen, *Biochim. Biophys. Acta* **2013**, *1828*, 528–534.
- [70] E. Strandberg, J. A. Killian, *FEBS Lett.* **2003**, *544*, 69–73.

Manuscript received: October 20, 2022  
Revised manuscript received: November 30, 2022  
Accepted manuscript online: December 1, 2022  
Version of record online: ■■■, ■■■■

## RESEARCH ARTICLE

A re-alignment of the short cationic helical peptide BP100 in membranes was detected by using solid-state  $^{19}\text{F}$ ,  $^{15}\text{N}$  and  $^2\text{H}$  NMR spectroscopy as well as MD simulations. High peptide concentration and temperatures just above the lipid phase transition promoted a flip from a surface-bound to transmembrane alignment. The inserted state was also favored by thin DLPC bilayers and by the presence of curvature-inducing lysolipids.



*Dr. E. Strandberg\**, *Dr. P. Wadhvani*,  
*Dr. J. Bürck*, *Dr. P. Anders*, *Dr. C. Mink*,  
*Dr. J. van den Berg*, *R. A. M. Ciriello*,  
*Dr. M. N. Melo*, *Prof. Dr. M. A. R. B.*  
*Castanho*, *Prof. Dr. E. Bardají*,  
*Prof. Dr. J. P. Ulmschneider*,  
*Prof. Dr. A. S. Ulrich\**

1 – 19

**Temperature-Dependent Re-alignment of the Short Multifunctional Peptide BP100 in Membranes Revealed by Solid-State NMR Spectroscopy and Molecular Dynamics Simulations**

